DNA 4279T

AIRCRAFT RESPONSE EFFECT ON E-FIELD MEASUREMENTS

R & D Associates

4640 Admiralty Way

Marina del Rey, California 90291

9 March 1977

Topical Report

CONTRACT No. DNA 001-77-C-0012

APPROVED FOR PUBLIC RELEASE;
DISTRIBUTION UNLIMITED.

Prepared for

Director

DEFENSE NUCLEAR AGENCY

Washington, D. C. 20305

REPORT DOCUMENTATION PAGE		READ INSTRUCTIONS BEFORE COMPLETING FORM
1. REPORT NUMBER DNA 4279T	2. GOVT ACCESSION NO.	3. RECIPIENT'S CATALOG NUMBER
4. TITLE (and Subtitle) AIRCRAFT RESPONSE EFFECT ON E-FIELD MEASUREMENTS		5. TYPE OF REPORT & PERIOD COVERED Topical Report
		6. PERFORMING ORG. REPORT NUMBER RDA-TR-140801-008
7. AUTHOR(s) Gerard K. Schlegel		8. CONTRACT OR GRANT NUMBER(s) DNA 001-77-C-0012
9. PERFORMING ORGANIZATION NAME AND ADDRESS R & D Associates 4640 Admiralty Way Marina del Rey, California 90291		10. PROGRAM ELEMENT, PROJECT, TASK AREA & WORK UNIT NUMBERS Subtask P99QAXDB001-24
11. CONTROLLING OFFICE NAME AND ADDRESS Director Defense Nuclear Agency Washington, D.C. 20301		12. REPORT DATE 9 March 1977
		13. NUMBER OF PAGES 88
14. MONITORING AGENCY NAME & ADDRESS(if different from Controlling Office)		15. SECURITY CLASS (of this report) UNCLASSIFIED
		15a. DECLASSIFICATION/DOWNGRADING SCHEDULE

16. DISTRIBUTION STATEMENT (of this Report)

Approved for public release; distribution unlimited.

17. DISTRIBUTION STATEMENT (of the abstract entered in Block 20, if different from Report)

18. SUPPLEMENTARY NOTES

This work sponsored by the Defense Nuclear Agency under RDT&E RMSS Code B310077464 P99QAXDB00124 H2590D.

19. KEY WORDS (Continue on reverse side if necessary and identify by block number)

Antenna Effective Height
Electric Field Measurements
CW Phase Calculations

20. ABSTRACT (Continue on reverse side if necessary and identify by block number)

This report describes the effect of the aircraft response on the measurement of E-fields. In investigating this effect, the effective height data developed by the Boeing Corporation for a 1-m blade antenna on a C-130 aircraft was utilized. Difficulties in using this data are discussed, and calculated phase functions to correspond to the amplitude data are presented. Calculated antenna open circuit voltages are then presented for different free field variations and polarizations.

DD FORM 1473 EDITION OF 1 NOV 65 IS OBSOLETE
1 JAN 73
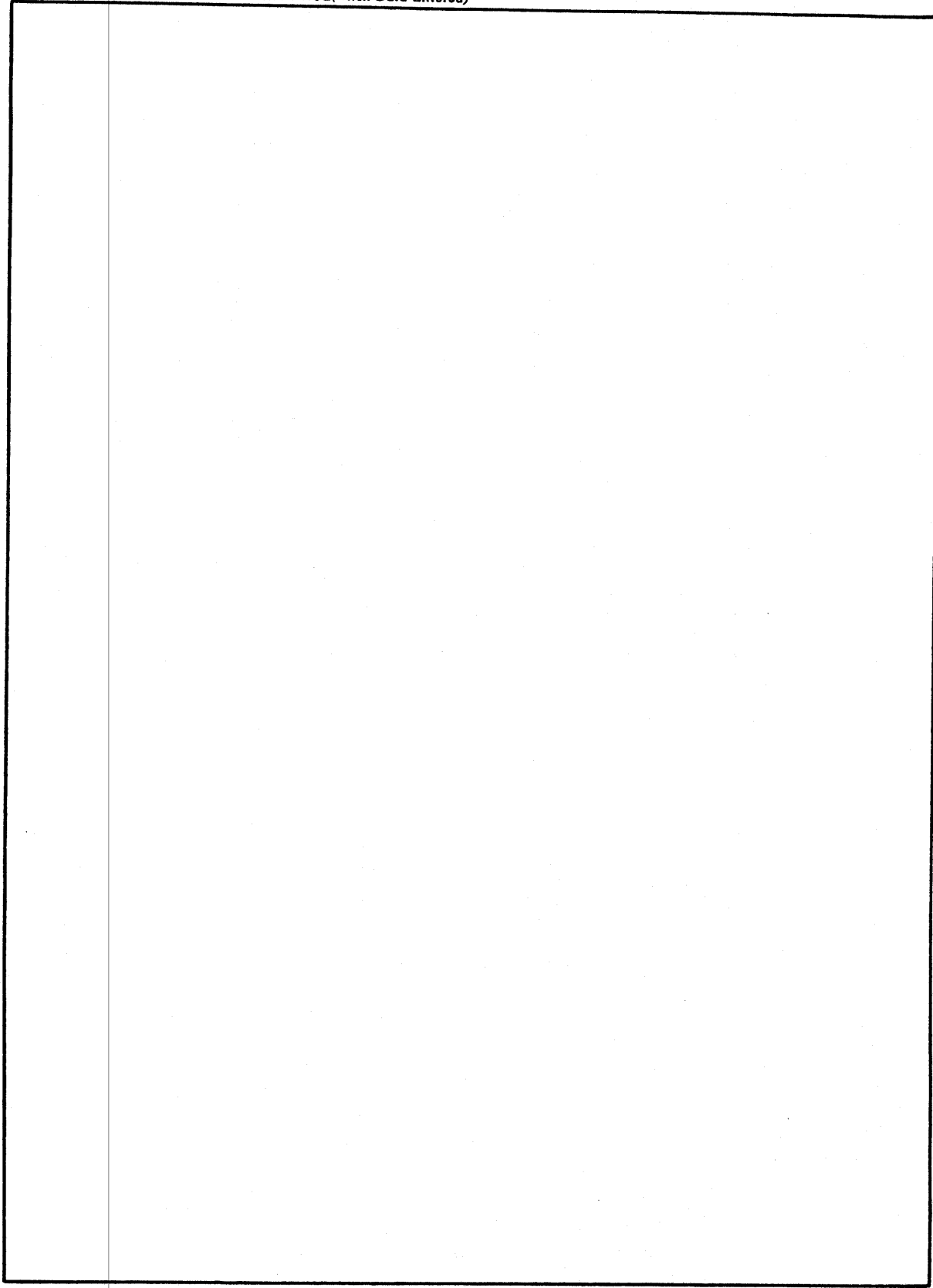
PREFACE

We wish to acknowledge the valuable suggestions and critical discussions provided by W. J. Karzas during the performance of this study.

TABLE OF CONTENTS

LIST OF FIGURES

LIST OF FIGURES (Continued)

4

LIST OF FIGURES (Continued)

SECTION I

INTRODUCTION

For a number of years, people have been concerned about the accuracy of electric field measurements made from antennas on aircraft. This concern has primarily been directed at the distortions in the field at the antenna caused by the presence of the aircraft.

In 1975, the Boeing Company under contract with the Defense Nuclear Agency (DNA) measured the complex effective height (h_e) for a one meter blade antenna on a C-130 aircraft. The experimental procedures and estimates of the accuracy of these measurements are dicussed in Reference 1 and will not be repeated here except to the extent necessary to indicate certain difficulties in using that data.

The purpose of these measurements was to ascertain the effect of the C-130 aircraft response on free field electromagnetic field measurements. Knowing the antenna effective height $(h_e(\omega))$ and the transfer function for the antenna delay line and oscilloscope circuit $(T(\omega))$, one can relate the scope voltage $(V_s(\omega))$ to the free space electric field in the frequency domain $(E(\omega))$ by the formula

$$V_s(\omega) = T(\omega) \cdot h_e(\omega) \cdot E(\omega). \tag{1}$$

A complexity is added when one considers the polarization of the electric field; however, using the principle of superposition, one can handle polarization effects in the plane perpendicular to the direction of propagation of the incident field. For this reason both the vertical (E aligned along the antenna axis) and the horizontal (E aligned along the fuselage axis) effective heights were measured. Thus for an incident field (E)-polarized at an angle α with respect to the antenna axis, Eq. 1 becomes

$$V_s(\omega) = T(\omega) \cdot [h_e(\omega)_v \cdot \cos \alpha + h_e(\omega)_h \cdot \sin \alpha] \cdot E(\omega). \tag{2}$$

To represent the effect of these transfer functions in the time domain, the procedure is as follows: First, the free field is transformed to the frequency domain by

$$E(\omega) = \int_{0}^{\infty} dt\ e^{i\omega t} E(t). \qquad (3)$$

Then, Eq. 2 is used and the inverse Fourier transform of $V_s(\omega)$ is taken as shown in Eq. 4:

$$V_s(t) = \int_{-\infty}^{\infty} \frac{d\omega}{2\pi} \cdot T(\omega) \cdot [h_e(\omega)_v \cdot \cos\alpha + h_e(\omega)_h \cdot \sin\alpha] \cdot E(\omega) \cdot e^{-i\omega t}. \qquad (4)$$

In this report, the transfer function for the antenna and equipment was assumed to be unity, and just the effect of the aircraft response investigated, utilizing Eq. 4. While implementing this equation seems straightforward, difficulties were encountered because the effective heights reported in Reference 1 were non-causal. These difficulties are discussed in Section II along with calculated phase functions for the effective heights that do preserve causality. In Section III, effective height functions utilizing the Boeing amplitude data and calculated phases were used to show the effect of the aircraft response on vertical, horizontal and 30° polarized incident fields. Conclusions are drawn in Section IV about the quality of electric field measurements made using the C-130 aircraft antenna. Additional discussions concerning the theory of amplitude and phase relationships, the difficulties with the measured effective heights and the complexity of estimating effective heights for antennas on ground planes are contained in the appendices.

SECTION II

AIRCRAFT RESPONSE TRANSFER FUNCTIONS

In the Boeing measurement program [1] both the amplitude and phase of the complex antenna effective height were measured. The estimated errors associated with these measurements were $\pm 2dB$[*] for the amplitude and $\pm 30°$ for the phase. However, there was an additional ambiguity associated with the data reduction of the phase which allowed any phase points to differ by $\pm 180°$ and any of the scaled frequency regions to differ by $\pm 90°$ [2]. It was due to this ambiguity that phase data were revised between the preliminary draft [3] and the final report [1] to provide correlation between the vertical, horizontal and 45° data. (See Appendix B.)

The major difficulty with using the effective heights reported is that they appear to be non-causal. This non-causal result is primarily attributed to inaccuracies in the phase.

As an example of the problems associated with using a non-causal effective height, consider Eq. 4 where $T(\omega) = 1$ and $\alpha = 0°$. Then,

$$V_s(t) = \int_{-\infty}^{\infty} \frac{d\omega}{2\pi} e^{-i\omega t} h_e(\omega) \cdot E(\omega). \qquad (5)$$

Equation 5 can be reduced to a convolution integral with

$$V_s(t) = \int_{0}^{\infty} dt' \cdot E(t') \cdot h_e(t-t') \qquad (6)$$

where $E(t) = 0$ for $t < 0$.

Now, if $h_e(t)$ is causal, then $h_e(t) = 0$ when $t < 0$, so the upper limit on Eq. 6 would be t. However, if $h_e(t) \neq 0$ when $t < 0$,

---

[*]dB error is defined as $dB = 20 \log_{10} \frac{(A \pm \varepsilon)}{A}$.

[1] Antenna Effective Length Measurement, The Boeing Company, Seattle, Washington, DNA 3798F-1,2, July 1975.

[2] Letter from D. D. Connell (Boeing) to Major W. Adams, DNA dated 23 September 1975.

[3] Antenna Effective Length Measurement, The Boeing Company, Seattle, Washington, D180-18878-1,2, July 1975 (draft).

then there are contributions to $V_s(t)$ from the integration of $t' > t$
or an error is introduced of the order

$$\varepsilon(V_s) = \int_t^\infty dt' \cdot E(t') \cdot h_e(t-t').$$ (7)

Physically, this means that the antenna is responding before
the field has arrived which is impossible. Figure 1 shows the function
$h_e(t)$ as computed from the Boeing data for the vertical and horizontal
data, and one can note the extent of the precursor for $t < 0$. The pro-
cedure for calculating $h_e(t)$ is explained in Appendix B. To correct
this deficiency, one could force the function $h_e(t)$ to zero at $t = 0$
and use a convolution integral. However, aside from the practical
problem of needing to perform N^2 calculations for a waveform out to
$t = N \cdot \Delta t$, there is the more important question of the accuracy of such
a forced calculation.

A more reasonable solution to this problem has been found by
assuming that the amplitude data is accurate to within the estimated
errors and then calculating a causal phase function. The theory for
relating amplitude and phase in a causal manner is discussed in Appendix
A. The results of these phase calculations are given in the following
subsections for both the vertical and horizontal polarizations.

2.1 VERTICAL EFFECTIVE HEIGHT

The amplitude data for the vertical effective height is shown
in Figure 2. The data was taken over the frequency range from 0.5 MHz
to 100 MHz with the dashed lines indicating the extrapolations used to
calculate the phase. This data shows that the low frequency effective
height is approximately half the physical height as opposed to a value
equal to the physical height which one would expect for an antenna over
a conducting ground plane.* This decrease for an expected value of 1 m
can be qualitatively explained by the simple models shown in Appendix
C.

_____

*In discussing effective heights of antennas over a ground plane one
must distinguish between the ratio of open circuit voltage to free
field versus open circuit voltage to free field plus reflected field.
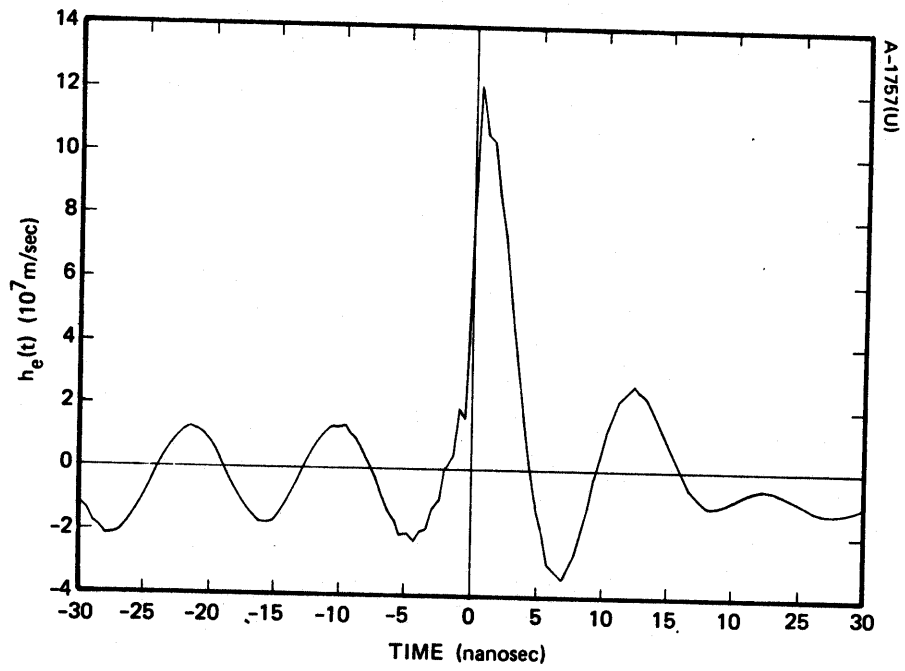For our effective heights we assumed the former.
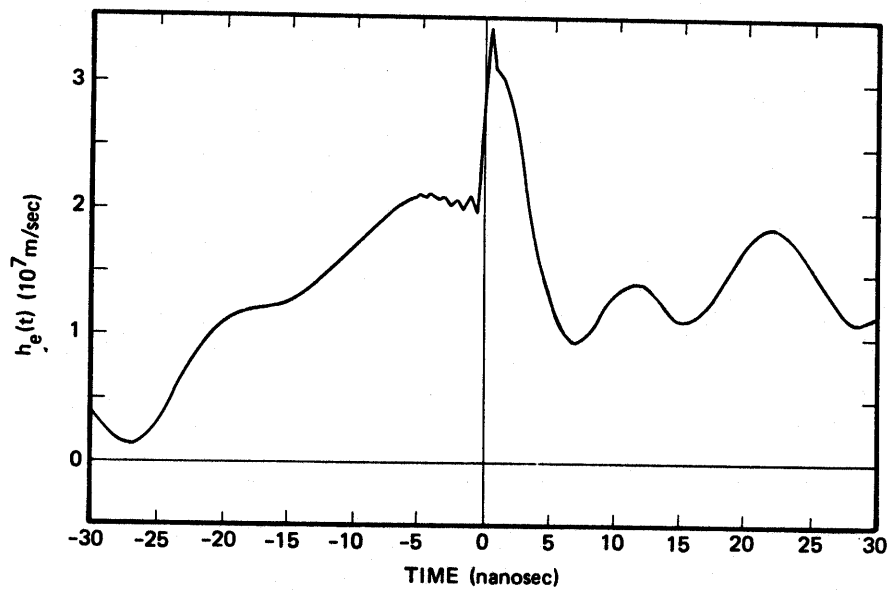
10

Figure 1a. $h_e(t)$ for the Vertically Polarized Data

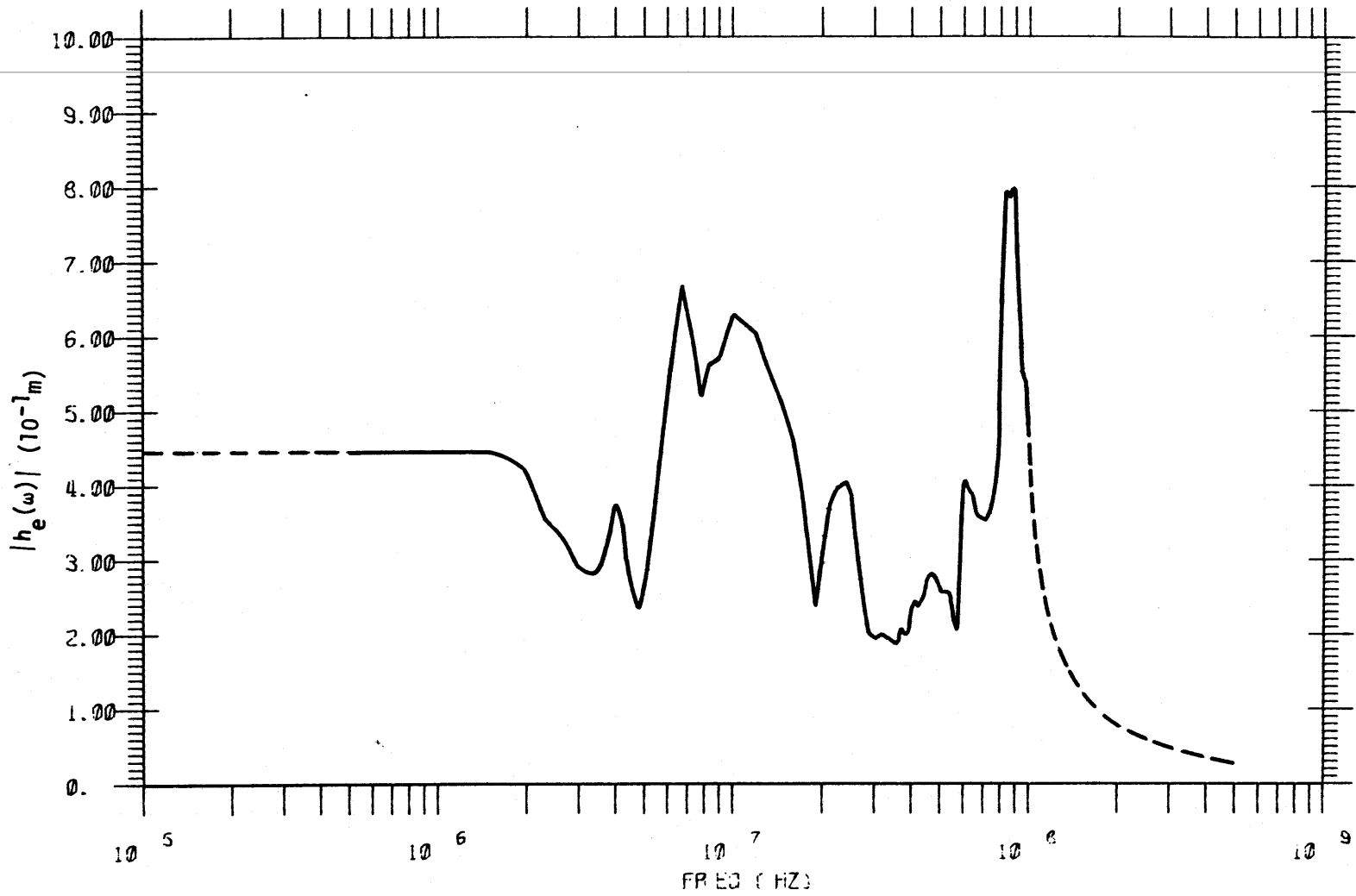Figure 1b. $h_e(t)$ for the Horizontally Polarized Data

11

12

Figure 2. $|h_e(\omega)|$ for Vertical Electric Field

Using this amplitude data, one can calculate a causal phase function from the formula derived in Appendix A. Namely,

$$\phi(\omega) = \phi_\infty(\omega) - \frac{2\omega}{\pi} \int_0^\infty \frac{dz}{(z^2 - \omega^2)} \quad \ln[A(z)/A_\infty(z)] - \ln[A(\omega)/A_\infty(\omega)] \ . \tag{8}$$

In order to use this equation we need to know how the amplitude data extrapolates to both $\omega = 0$ and $\omega = \infty$ and also what the phase value is for large ω.

For low frequencies, the effective height of a monopole antenna on a conducting surface goes to a constant value, as discussed in Appendix C. Thus, for $\omega < 2\pi \cdot (0.5 \text{ MHz})$

$$A(\omega) = A[2\pi \cdot (0.5 \text{ MHz})] . \tag{9}$$

For the high frequencies, we know that a dipole effective height falls off like $1/\omega$ and that a monopole over a ground plane is electrically/equivalent to a center fed dipole. Thus, we want our extrapolated function to have a $1/\omega$ dependence at very high frequencies. In addition, we want it to have a smooth transition from the measured data. As can be seen in Figure 2, there appears to be a resonance in the amplitude data at 85 MHz. This resonance can be fit by the form

$$A(\omega) = \frac{(0.8) \cdot \omega \cdot \Delta\omega}{[(\omega_0 - \omega^2)^2 + (\omega\Delta\omega)^2]^{1/2}} \tag{10}$$

where $\omega_0 = 2\pi \ (85 \text{ MHz})$

$\Delta\omega = 2\pi \ (85 \text{ MHz})$.

We note that for $\omega \gg \omega_0$, $A(\omega) \to 1_0/\omega$. Therefore, for $\omega > 2\pi \cdot (100 \text{ MHz})$ the amplitude was extrapolated using Eq. 10.

For a function whose amplitude decays as $1/\omega$, the phase changes by $\pi/2$ during that fall off (see Appendix A); thus, the phase infinity (ϕ_∞) is $\pi/2$.

These are the parameters and functions which were used to calculate the vertical phase function. It should be noted that the purpose of these extrapolations beyond the frequency band measured (.5 to 100 MHz) was not to gain information outside that band, but

13

rather to insure that we do not introduce non-physical, erroneous features in the applicable time transformed data.

The calculated phase function is shown in Figure 3. For comparison purposes, the measured phase data have also been plotted. One can note that other than the 180° phase shift at the beginning of the data the curves are in fair agreement, particularly when one considers the ±90° ambiguity on the measured data. Figure 4 and 5 show the delta and step function responses for the combined measured amplitude and calculated phase curves. As is shown in Appendix B, the complex effective height for the vertical polarization described by the amplitude data (Figure 2) and the calculated phase function (Figure 3) is now causal in the time domain.

2.2 HORIZONTAL EFFECTIVE HEIGHT

The ampltiude data for the horizontal effective height is shown in Figure 6. Again, the dashed lines represent the extrapolations used to calculate the phase. For this data we note that the effective height is equal to the physical height at the low frequencies. A simple model for the coupling of a horizontal field with a vertical antenna is shown in Appendix C and basically involves the coupling of the dipole field generated by the fuselage with the antenna. An important point to note is that the coupled voltage will change sign depending on which way the incident free field is polarized.

Using Equation 8 we have calculated a causal phase function. In performing this calculation we have used the following extrapolations for the amplitude data. For low frequencies, we again have a constant value which reflects the fairly constant charge distribution on the fuselage for frequencies below the fuselage resonance of ~ 2 MHz. Therefore, for $\omega < 2\pi(0.5$ MHz$)$

$$A(\omega) = A(2\pi \cdot 0.5 \text{ MHz}) \quad . \tag{11}$$

For high frequencies, we again note that the data shown in Figure 6 has a $1/\omega$ decay, which is consistent with a dipole created by the fuselage. Therefore, for frequencies above $(2\pi \cdot 100$ MHz$)$ we used the form

$$A(\omega) = \left[A(2\pi \cdot 100 \text{ MHz}) - \frac{\omega_0}{\omega_1} \right] \left(\frac{\omega_1}{\omega} \right)^{\omega} + \frac{\omega_0}{\omega} \tag{12}$$

14

Figure 3.   Phase of $h_e(\omega)$ for a Vertical Electric Field
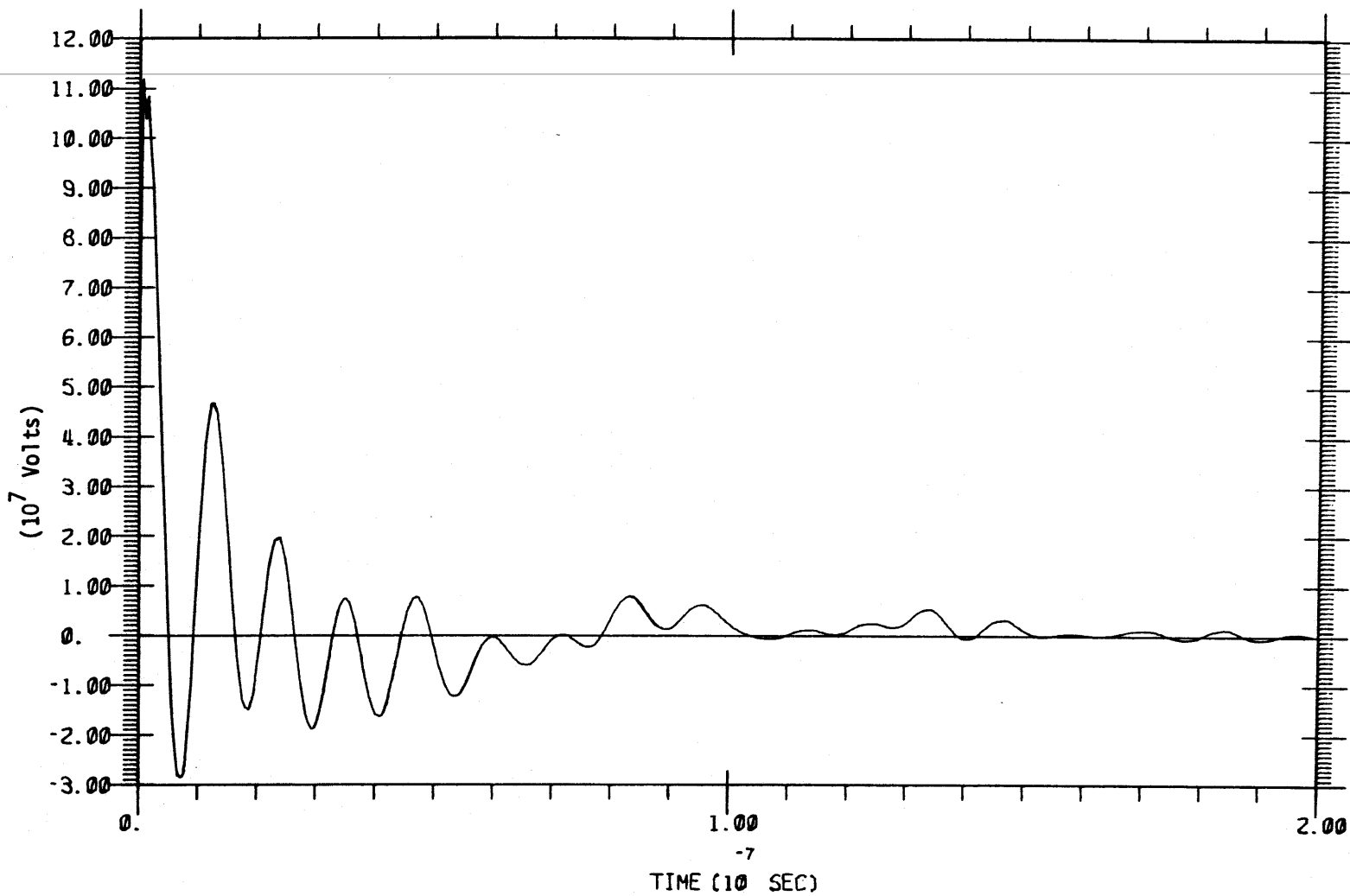
Figure 4.   Delta Function Response for Vertical Polarization
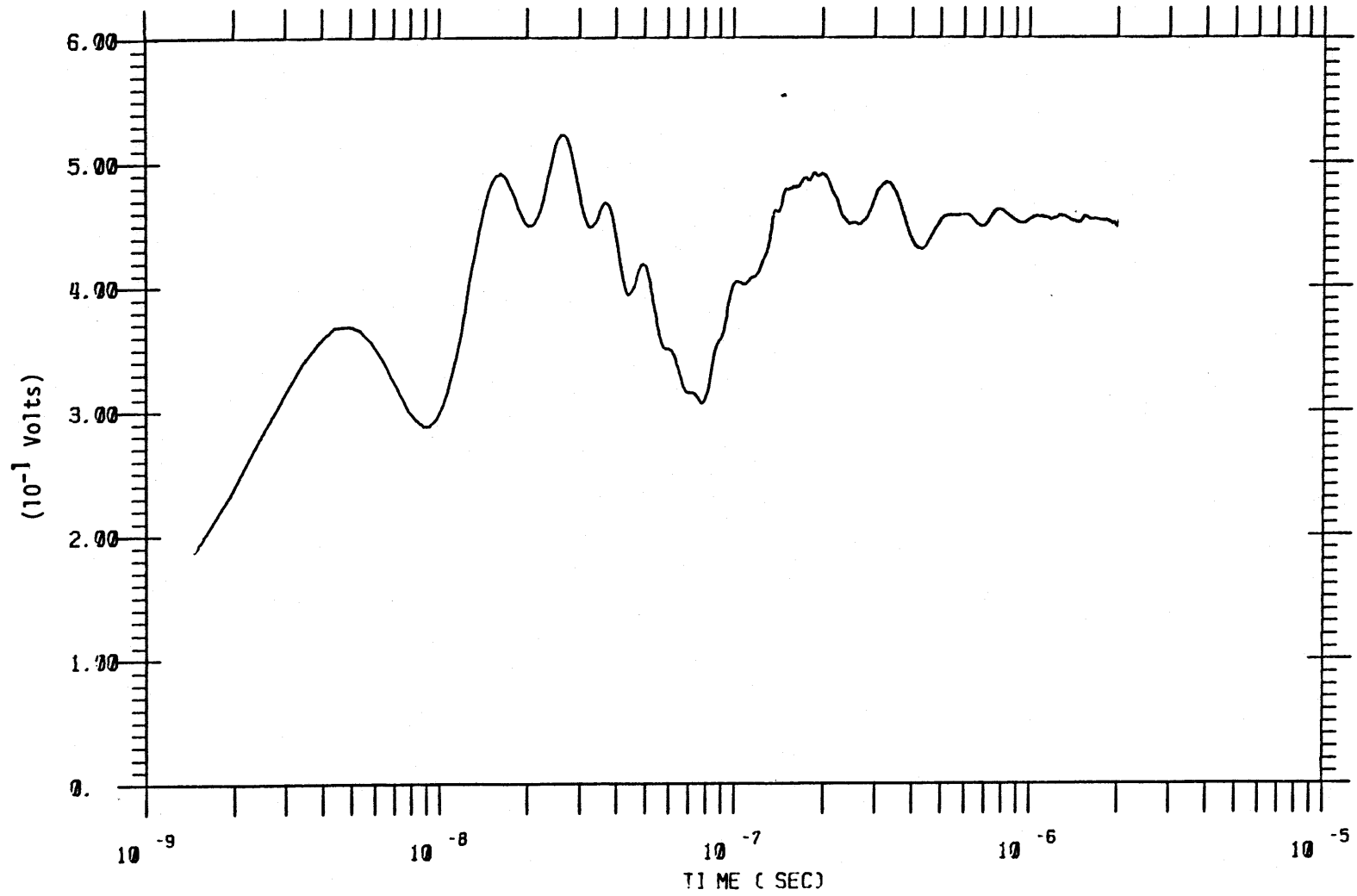
Figure 5. Step Function Response for Vertical Polarization
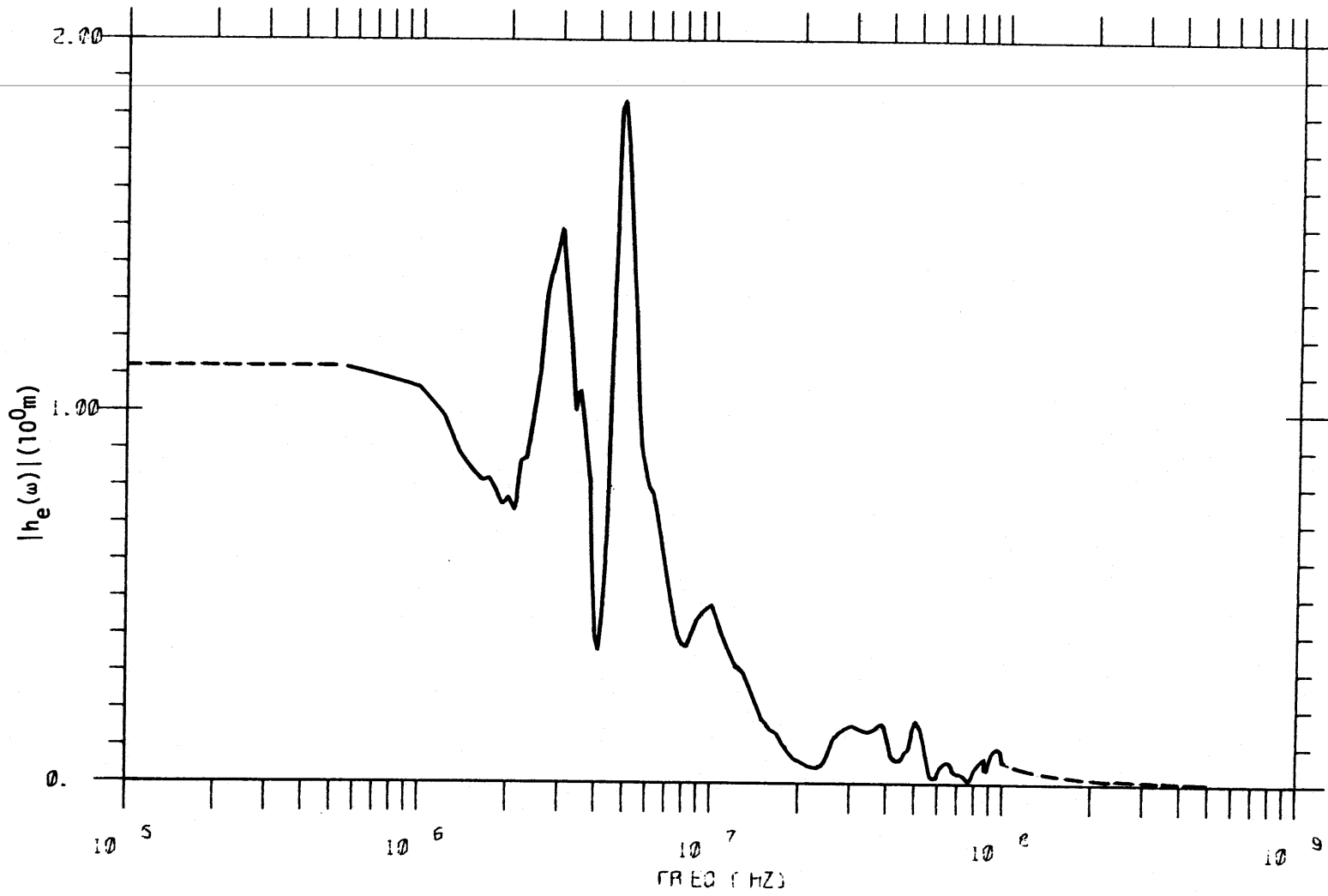
Figure 6. $|h_e(\omega)|$ for a Horizontal Electric Field

18

where $\omega_0 = 2$ MHz $\cdot$ 2π

$\omega_1 = 100$ MHz $\cdot$ 2π.

The first term in Eq. 12 provides a transition for the data to the high frequency form. Again, for a $1/\omega$ decay the phase changes by $\pi/2$, so $\phi_\infty = \pi/2$.

Figure 7 shows the calculated phase along with the measured phase data. At first glance there appears to be considerable difference; however, it should be noted that given the $\pm 30°$ accuracy of the data and the $\pm 90°$ ambiguity within scaled frequency bands (see Appendix B) the difference may not be as great. Figures 8 and 9 are graphs of the delta and step function response using the amplitude data and the calculated phase function.

As a further check on the accuracy of these new effective height functions, they have been used to predict the effective height for a $45°$ polarization and then compared with the measured data for $45°$. This comparison is discussed in Appendix B.
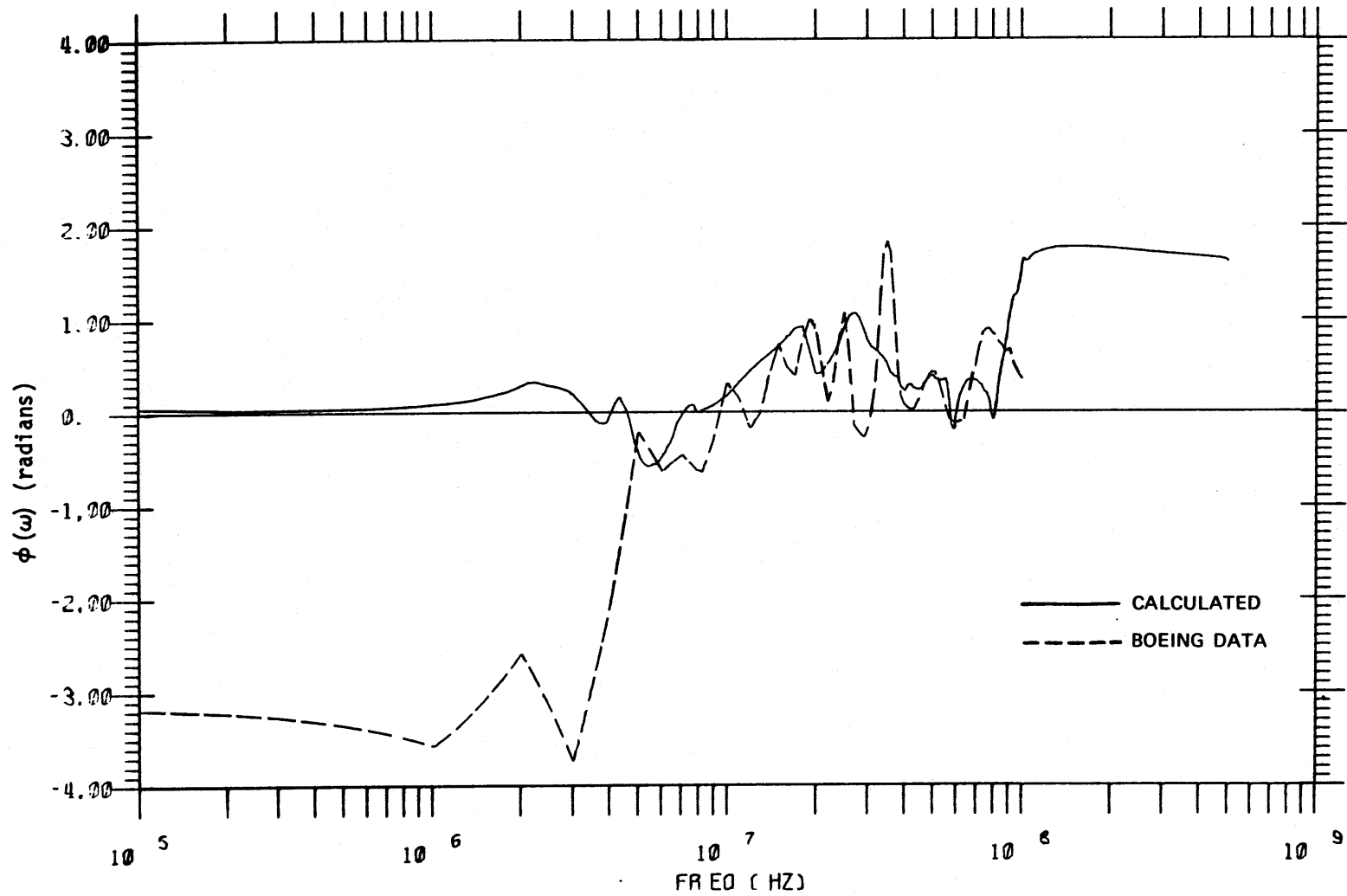
Figure 7. Phase of $h_e(\omega)$ for a Horizontal Electric Field
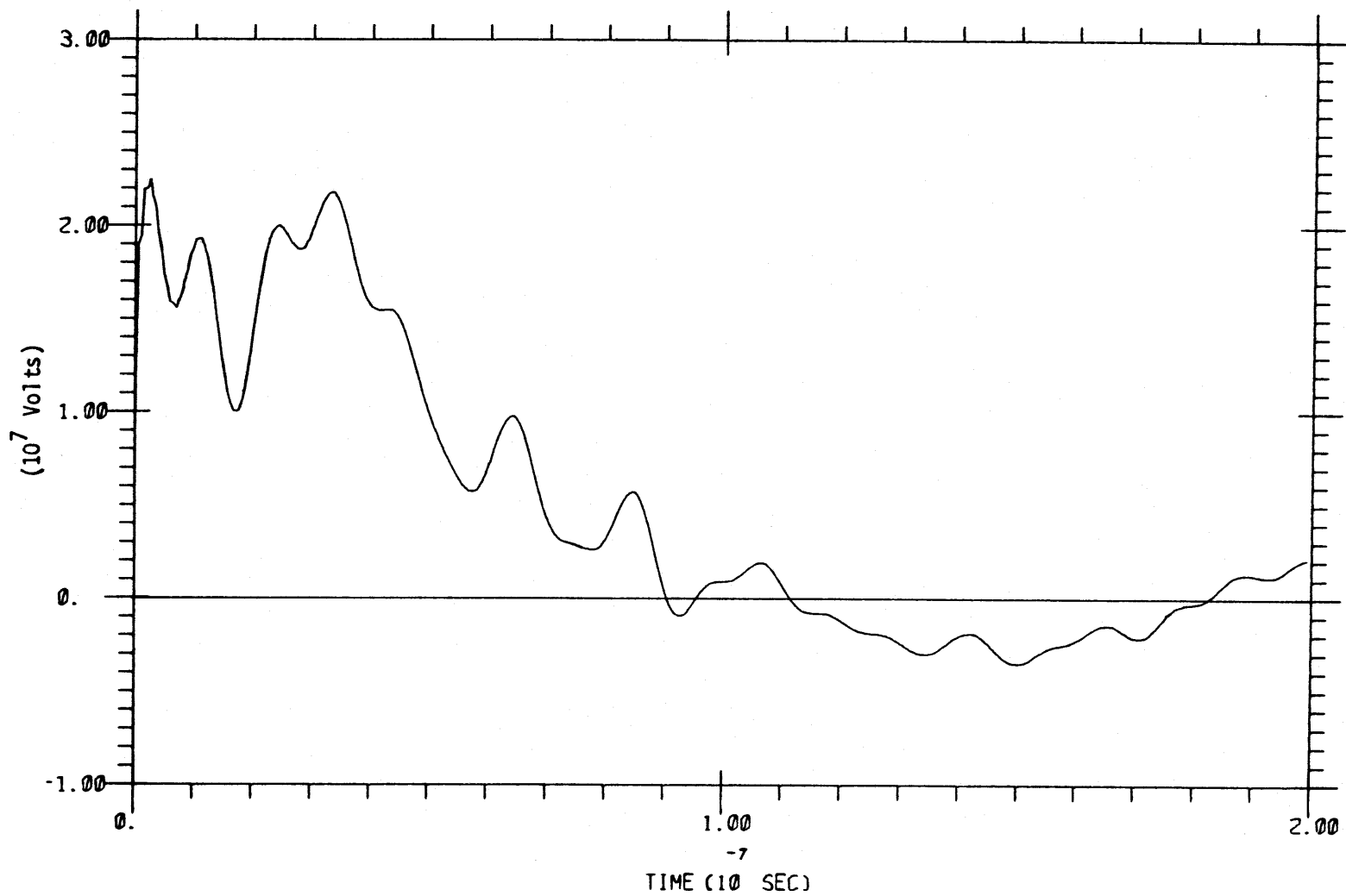
Figure 8. Delta Function Response for Horizontal Polarization

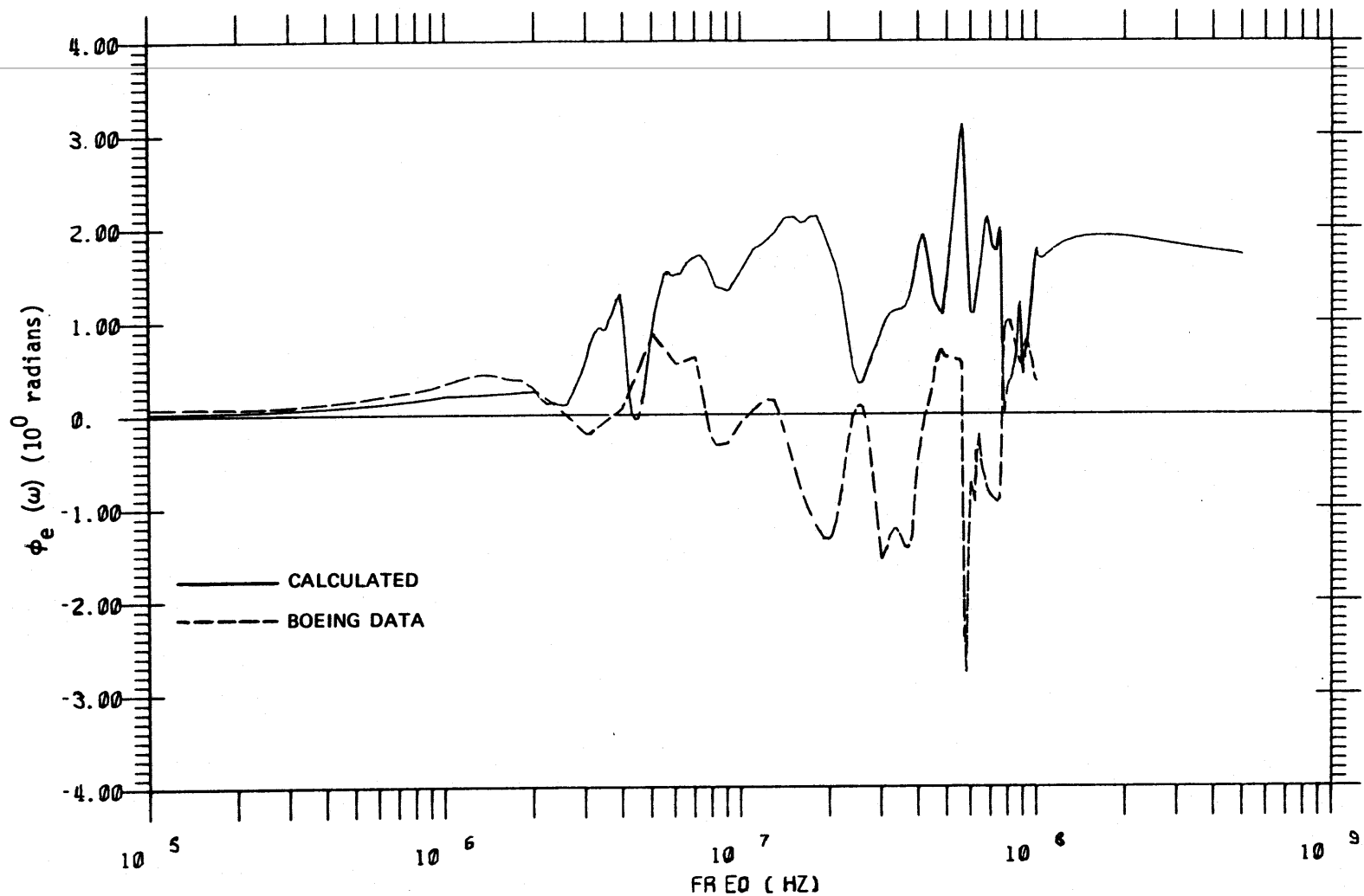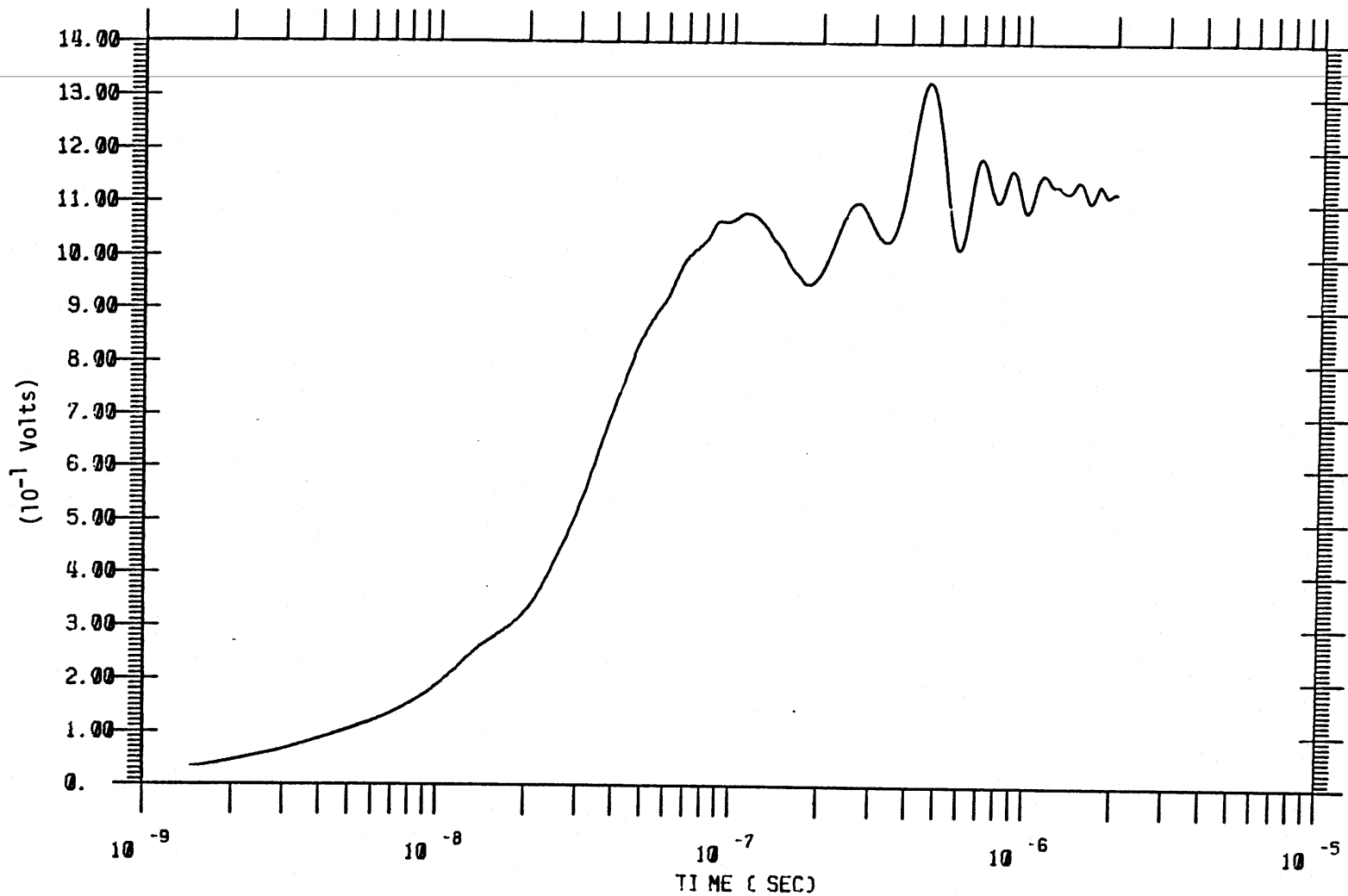Figure 9. Step Function Response for Horizontal Polarization

SECTION III.

EFFECT OF AIRCRAFT RESPONSE ON MEASUREMENTS

The effective height functions which were discussed in Section
II can be used to investigate the sensitivity of electric field
measurements made on such an aircraft platform. For the free field,
we have assumed an analytic function of the form

$$E(t) = E_o \frac{e^{a(t-T)}}{1 + e^{b(t-T)}} \quad . \tag{13}$$

The Fourier transform of such a function is

$$E(\omega) = \frac{E_o \pi}{b} \left\{ \frac{e^{i\omega T}}{\sin\left[\frac{\pi}{b}(a+i\omega)\right]} \right\} \quad . \tag{14}$$

The amplitude and phase are given by the following equations.

$$|E(\omega)| = E_o \frac{\sqrt{2}\pi}{b} \left[\cosh(2A) - \cos(2B) \right]^{-1/2} \tag{15}$$

and

$$\phi_E(\omega) = \omega T + \tan^{-1} \left[-\frac{\tanh(A)}{\tan(B)} \right] \tag{16}$$

where $A = \frac{\pi\omega}{b}$

$B = \frac{\pi a}{b} \quad .$

Figures 10 and 11 show the time waveform and its Fourier transform for
two sets of parameters, with the peak value normalized to one.

$$
\begin{aligned}
\text{Case 1)} \quad & a = 2.0 \times 10^8 \\
& b = 2.7 \times 10^8 \\
& T = 5.0 \times 10^{-8} \\[6pt]
\text{Case 2)} \quad & a = 2.0 \times 10^8 \\
& b = 2.1 \times 10^8 \\
& T = 5.0 \times 10^{-8}
\end{aligned}
$$

Using the above analytic form with both sets of parameters,
we have calculated the equivalent open circuit voltage at the antenna

23

Figure 10a.   Time Waveform of the Incident Field

Figure 10b.   Time Waveform of the Incident Electric Field

24

Figure 11a. $|E(\omega)|$ for the Incident Electric Fields

25

Figure 11b. Phase for the Incident Electric Fields

Eq. 1, for three electric field polarizations: (1) vertical, the E-field aligned along the antenna (2) horizontal, the E-field alig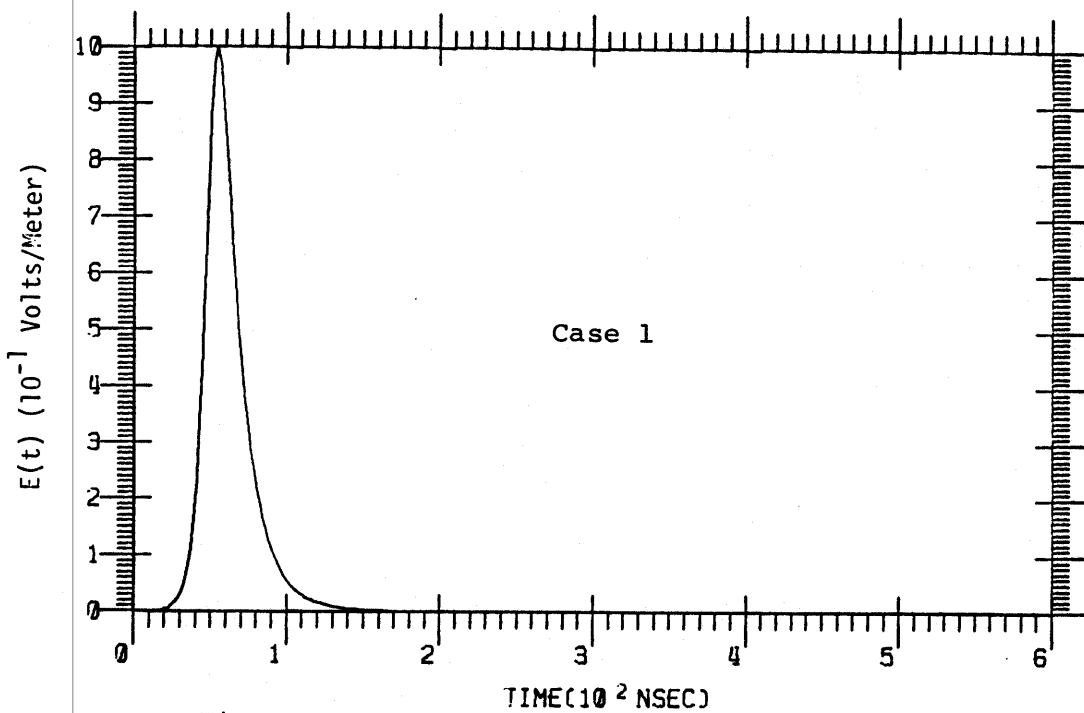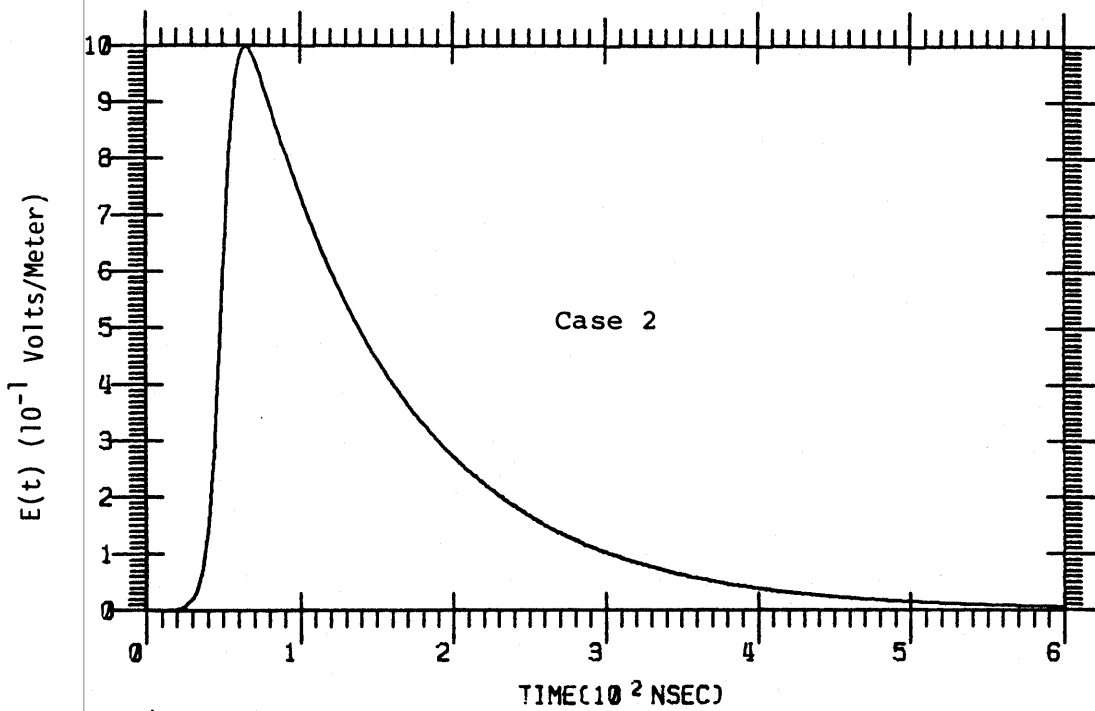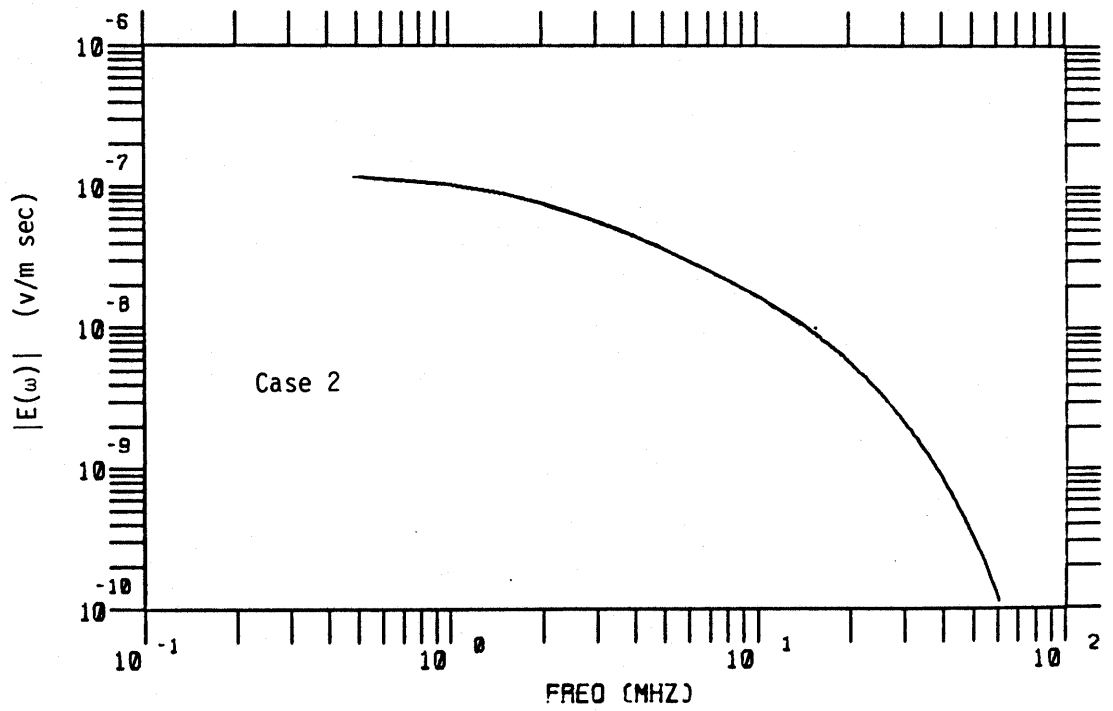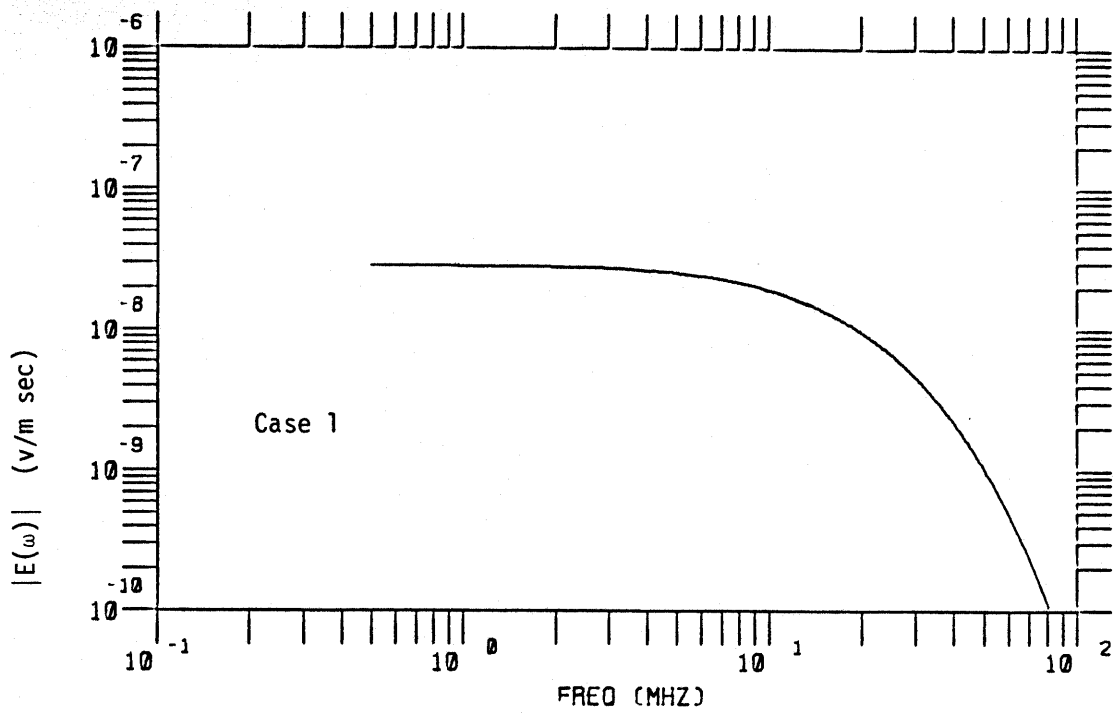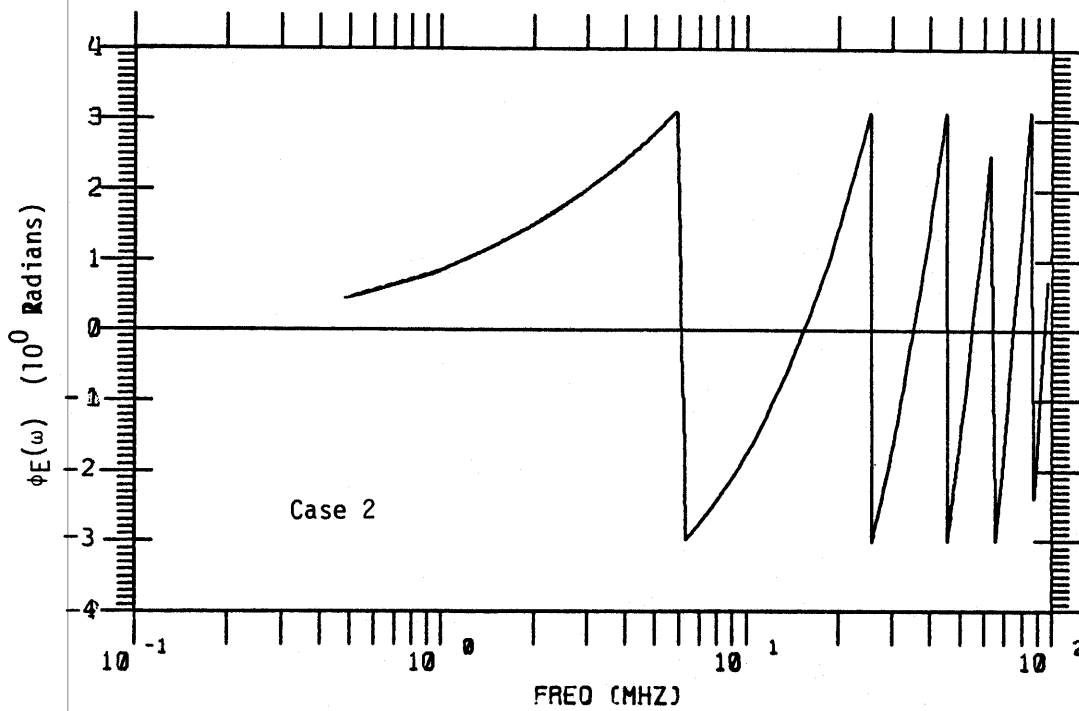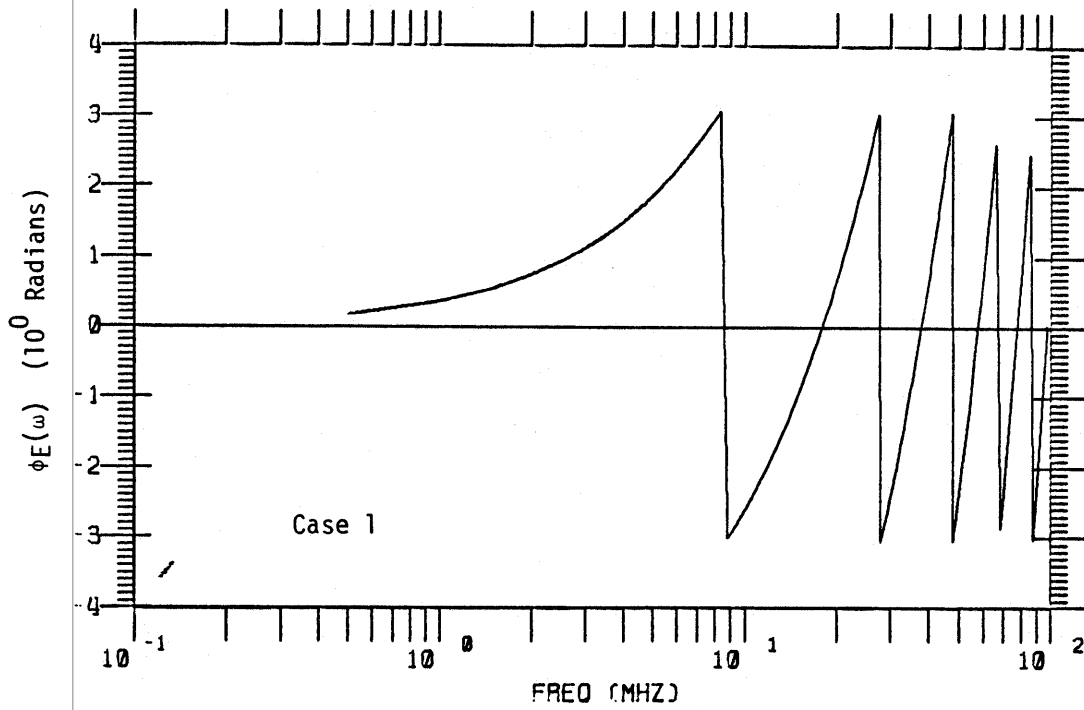ned along the fuselage, and (3) 30°, the E-field aligned at 30° with respect to the antenna and pointing toward the front of the aircraft. Figure 12 shows the orientation for each polarization.

3.1 VERTICAL POLARIZATION EFFECTS

The antenna open circuit voltage as a function of time for a case 1 vertical field is shown in Figure 13. Also overlaid on the graph is the voltage waveform that would have resulted if the effective height had been constant and equal to the physical height (1 m). We will refer to this waveform as the "free field voltage". This reduction in peak voltage below the one-half value expected from the low frequency effective height data is caused by the narrowness (high frequency nature) of the incident pulse. Figure 14a and 14b show similar calculations for the slower decaying pulse (lower frequency) of case 2. For this case the peak voltage is approximately 0.5 as expected. In both cases there is a rippling in the calculated voltage caused by the resonances in the effective height data at approximately 5 to 10 MHz.

3.2 HORIZONTAL POLARIZATION EFFECTS

For an incident electric field that is horizontally polarized there is still a voltage generated on the antenna. Figures 15a and 15b show the calculated antenna open circuit voltage for an incident field with case 1 parameters. Also shown in this graph for reference is the voltage that would be on the antenna if the field had been vertical and the effective height equal to the physical height (1 m). Note, for this polarization, the shape of the antenna voltage is much slower than the "free field voltage". For the slower decaying incident field of case 2 (Figures 16a and 16b), we note that the peak of the antenna voltage is significantly increased due to the larger low frequency content in the incident free field. In both cases we see there are oscillations caused by aircraft resonances. These calculations show that for an antenna mounted near the front of the fuselage there can be a strong contaminant signal on a vertical antenna from a horizontally polarized free field. This cross-polarized coupling is caused by the E field generated by charge distributions induced on the aircraft, notably the fuselage, and is basically a low frequency effect as shown in Appendix C. The effect of this cross coupling will

27
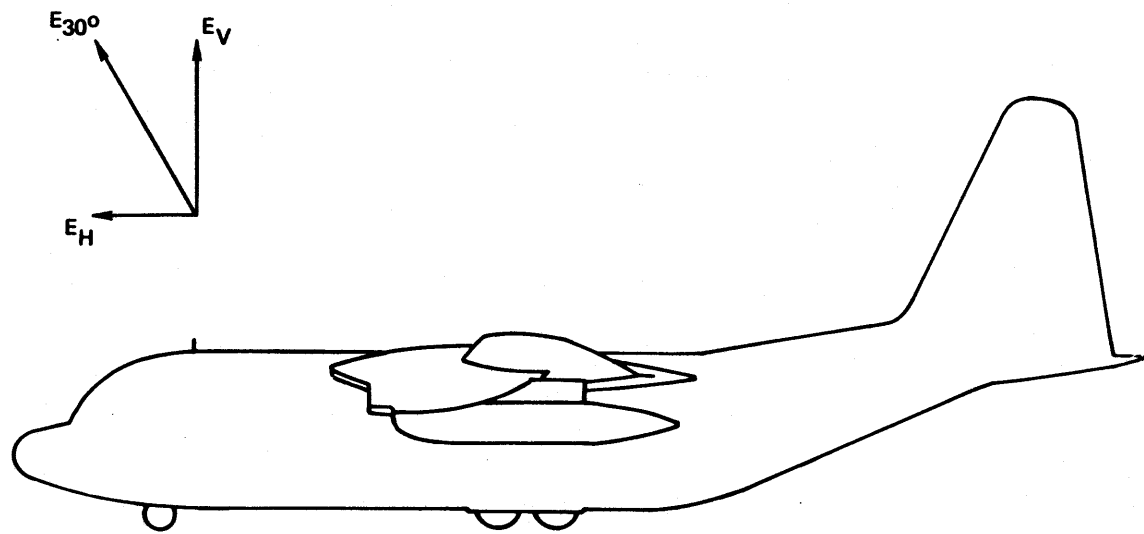
Figure 12.   E-field Polarization Relative to the Antenna and Aircraft
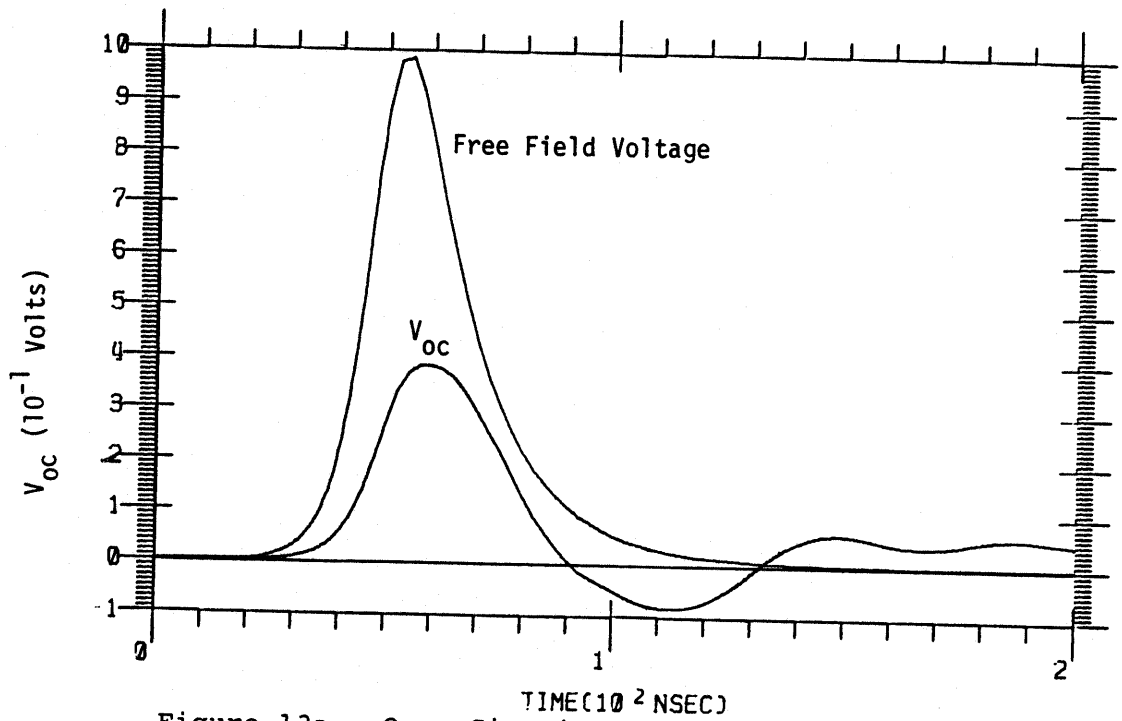
Figure 13a. Open Circuit Voltage for Vertical Case 1
Electric Field (200 nsec)
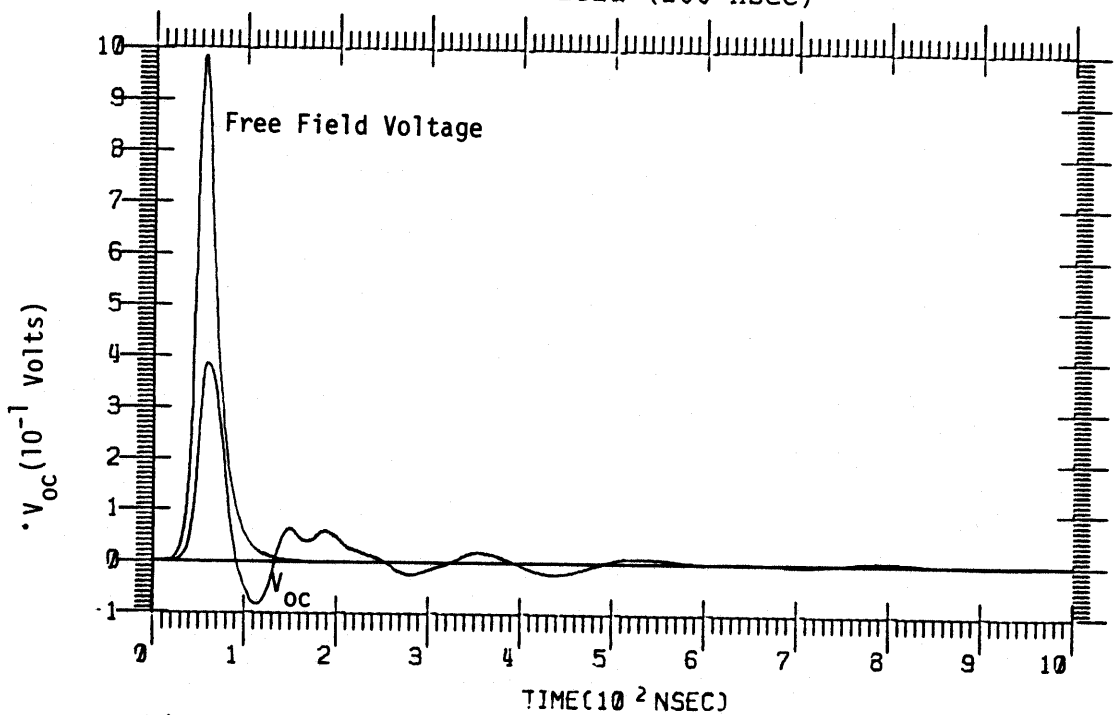
Figure 13b. Open Circuit Voltage for Vertical Case 2
Electric Field (1 μsec)
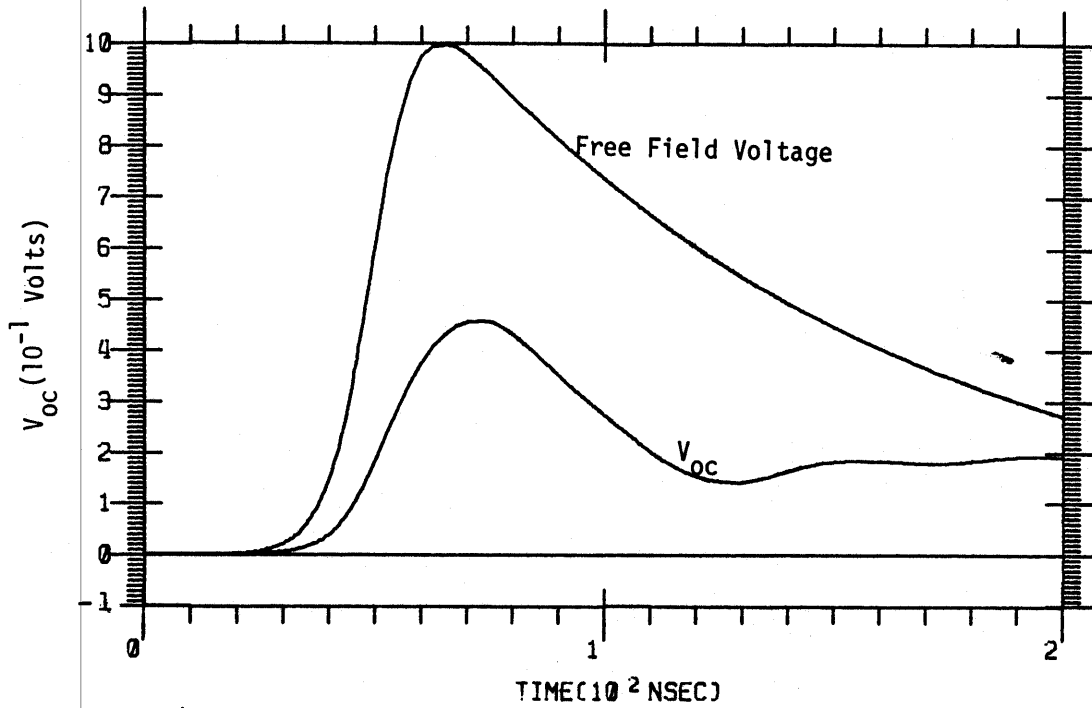
Figure 14a.   Open Circuit Voltage for Vertical Case 2
             Electric Field (200 nsec)
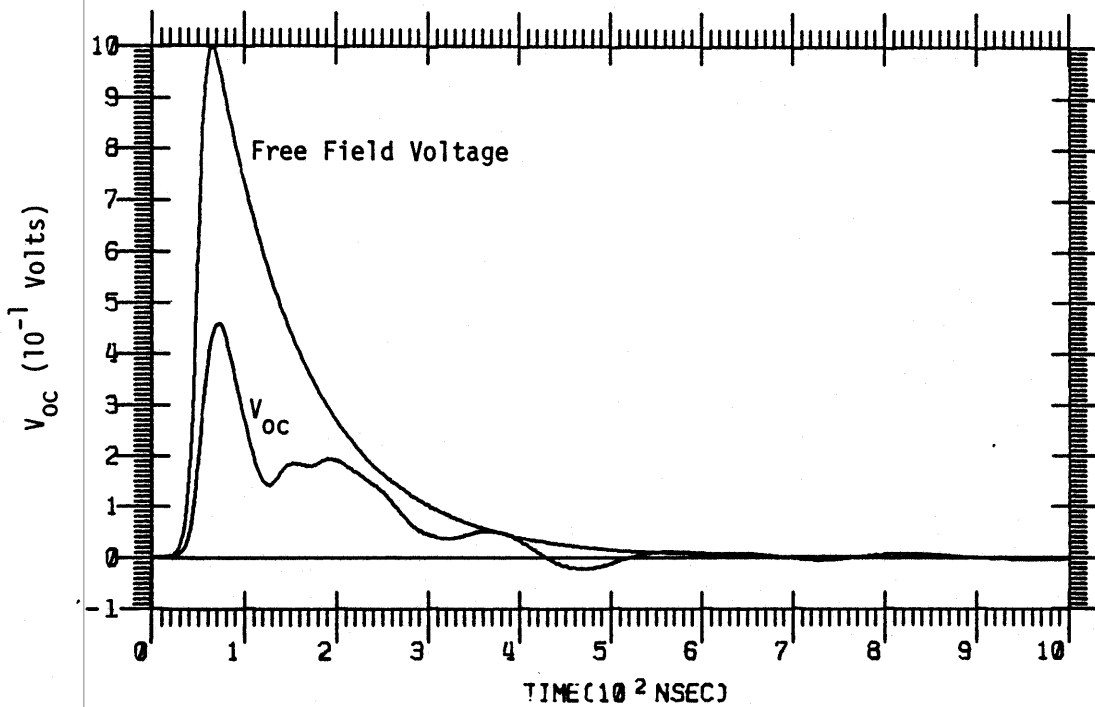
Figure 14b.   Open Circuit Voltage for Vertical Case 2
             Electric Field (1 μsec)

30

Figure 15a. Open Circuit Voltage for Horizontal Case 1 Electric Field (200 nsec)
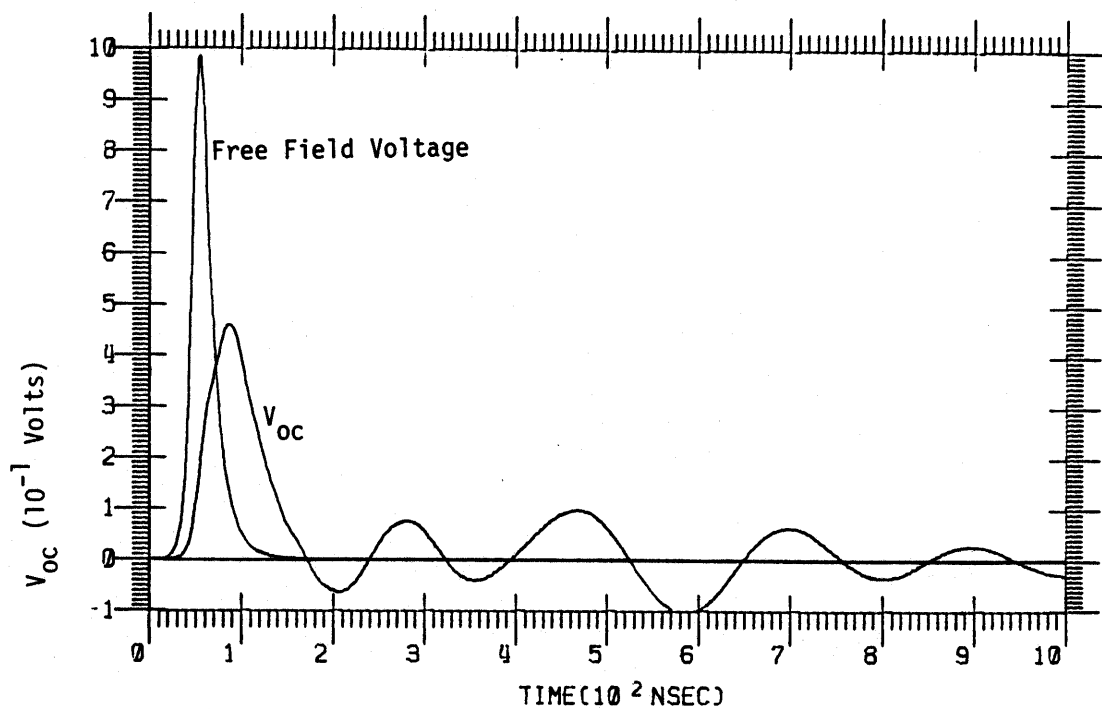
Figure 15b. Open Circuit Voltage for Horizontal Case 1 Electric Field (1 μsec)

31

Figure 16a.　Open Circuit Voltage for Horizontal Case 2
　　　　　　　Electric Field (200 nsec)
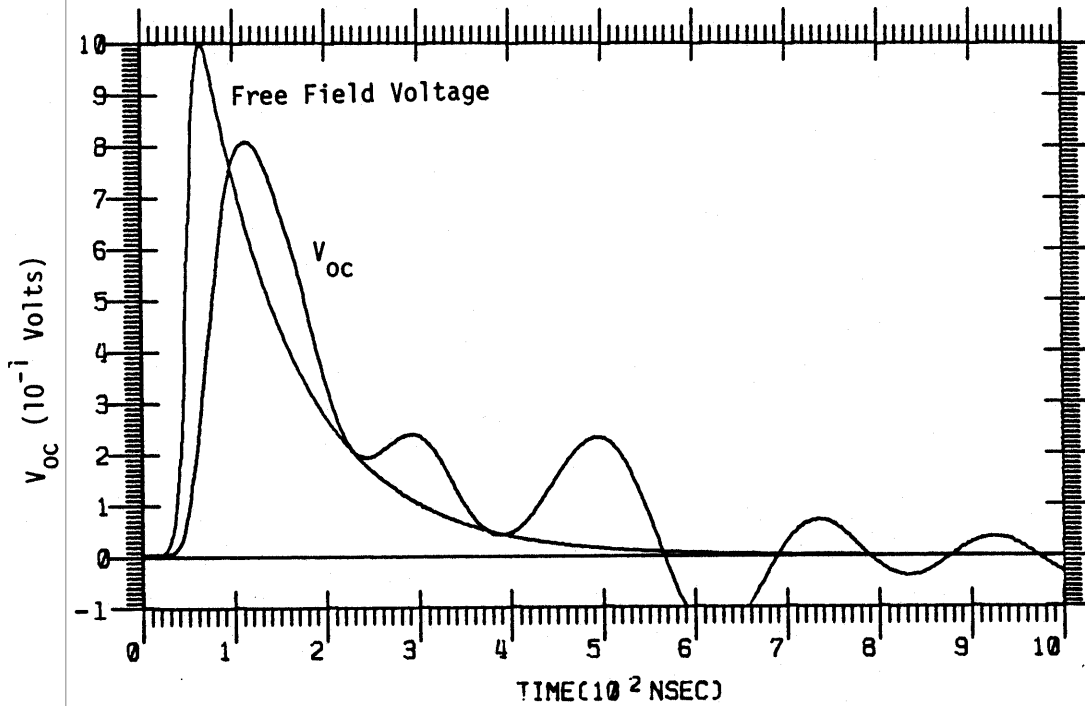
Figure 16b.　Open Circuit Voltage for Horizontal Case 2
　　　　　　　Electric Field (1 μsec)

be to distort any measurement of the vertical component of a free space field. The significance of this distortion can be seen by the following calculations for a free field polarized at 30° relative to the vertical.

3.3 30° POLARIZED FIELD

For a free field polarized at 30° to the vertical (see Figure 12) the antenna open circuit voltage is a combination of both the vertical component coupling directly with the antenna and the horizontal component cross coupling with the antenna by means of charge distributions induced on the aircraft body. In calculating the antenna open circuit voltage that results from such a polarized field, it is important to note the relative orientation of the vertical and horizonal components. In our calculation we have the field orineted 30° from the vertical in the forward (referenced to the aircraft) direction. For this orientation, the antenna voltages for both the vertical and horizontal components add, and the results are shown in Figures 17a and 17b for case 1 and in Figure 18a and 18b for case 2. However, had we oriented the field 30° from the vertical in the aft direction, then the antenna voltage from the horizontal component of the field would be opposite in sign from that seen by the vertical component and some cancellation would have resulted.

For comparison, the voltage that the vertical component alone would have generated with an antenna effective height equal to the physical height has also been plotted on the graphs. In observing Figures 17 and 18, we see that the antenna open circuit voltage is considerably different in shape from the free field voltage. This distortion has been mainly caused by the cross coupling of the horizontal component of the field with the antenna.

The point to be made from these calculations is that because of the frequency dependence of the effective height and because of the cross coupling of the horizontal component of the incident field, the recorded voltage from a monopole antenna on an aircraft does not adequately measure the vertical component of an incident electric field.
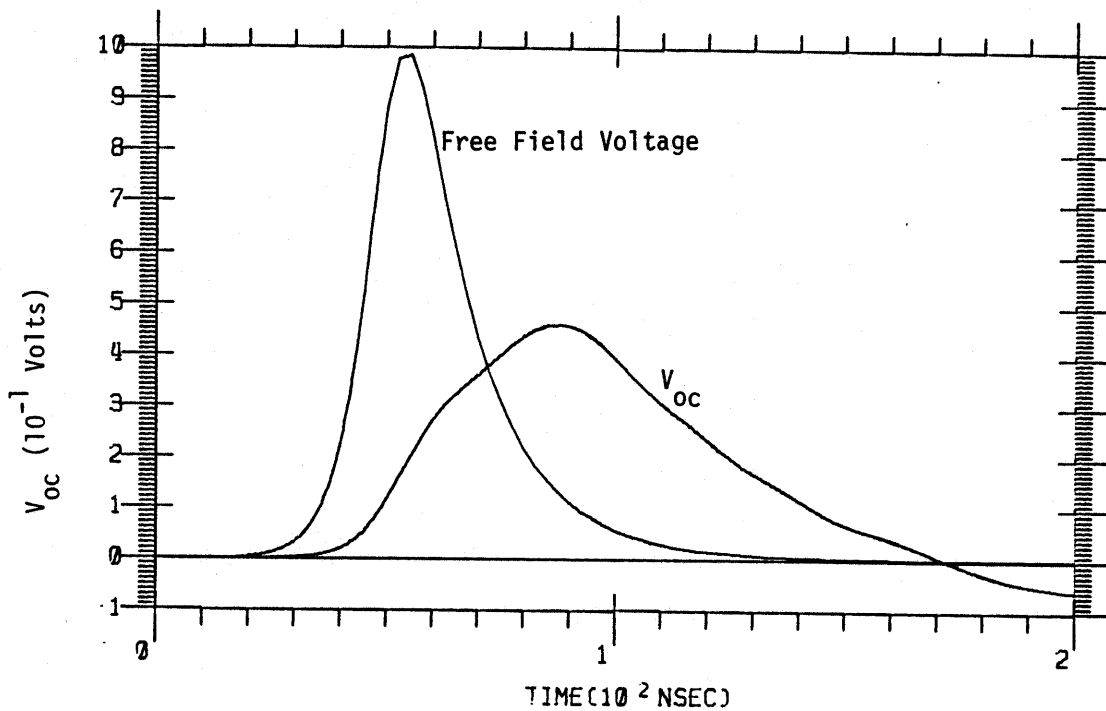
Figure 17a. Open Circuit Voltage for 30° Polarized Case 1
Electric Field (200 nsec)
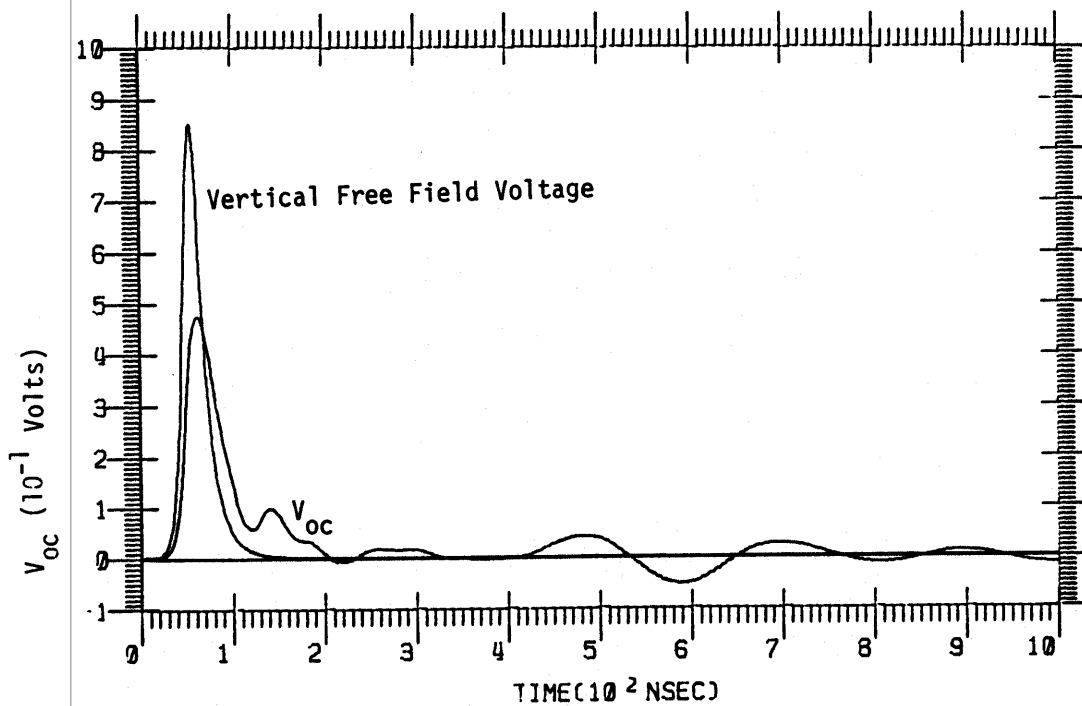
Figure 17b. Open Circuit Voltage for 30° Polarized Case 1
Electric Field (1 µsec)
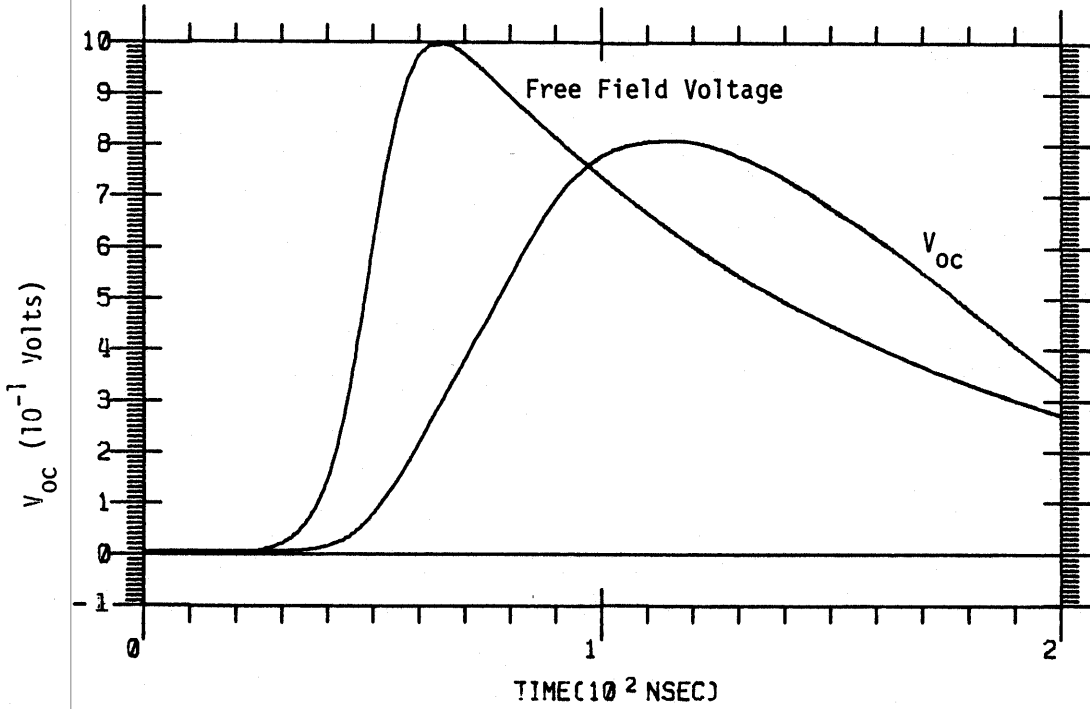
34
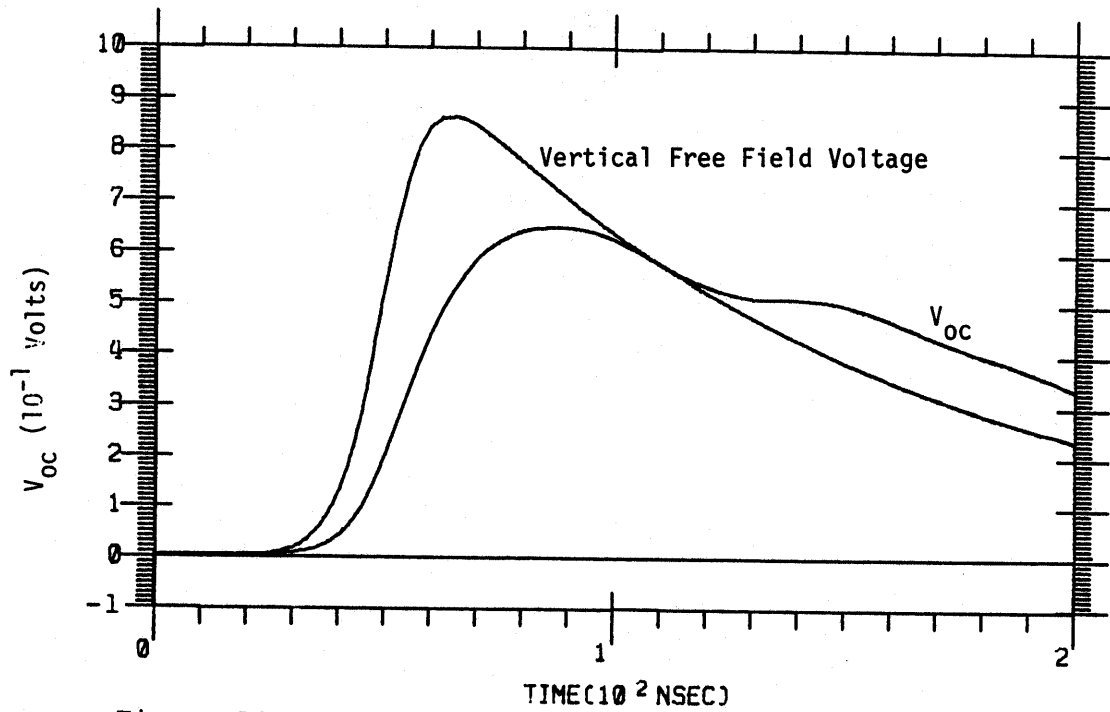
Figure 18a.   Open Circuit Voltage for 30° Polarized Case 2
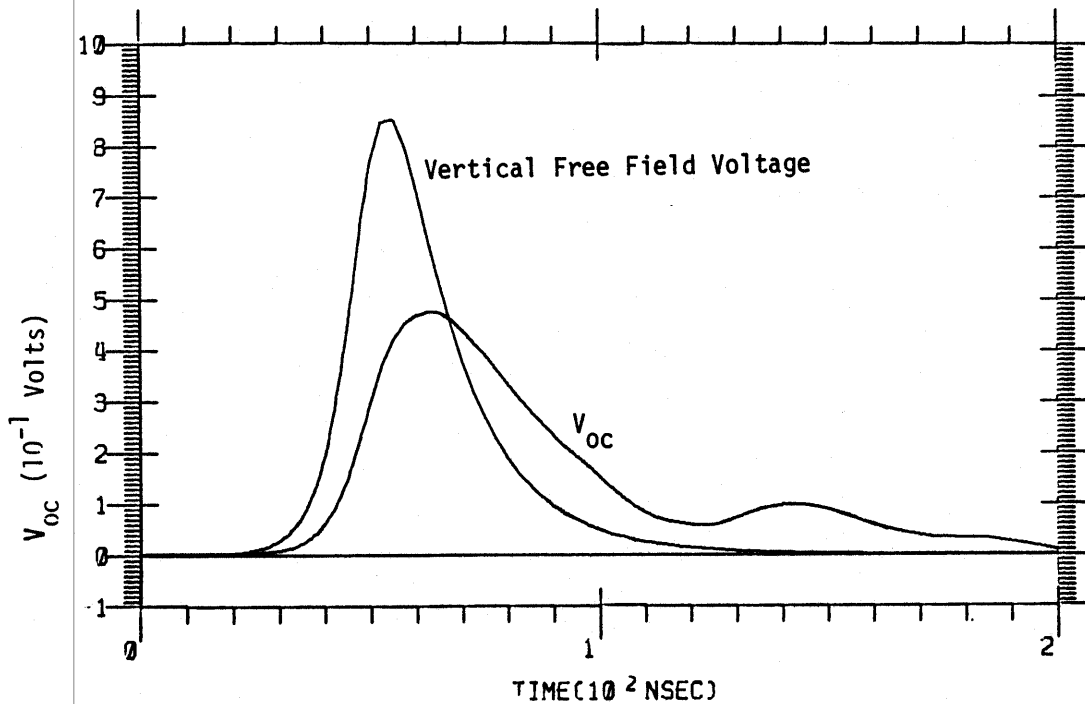   Electric Field (200 nsec)
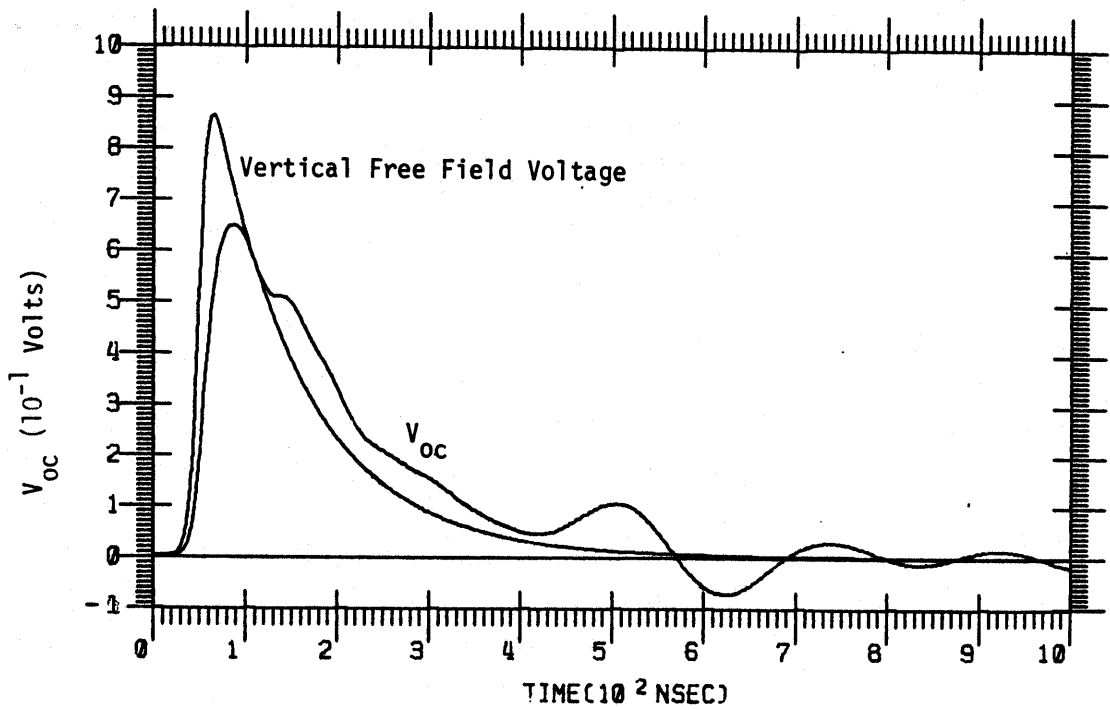
Figure 18b.   Open Circuit Voltage for 30° Polarized Case 2
              Electric Field (1 μsec)

35

SECTION IV.

CONCLUSIONS

Our ability to make accurate electric field measurements from
aircraft platforms has been questioned because of two contaminating
effects, which are referred to as the aircraft response. First, the
enhancement of the normal electric field by the conducting surface of
the aircraft is affected by the finite dimensions of the aircraft and
is not readily known. Second, there is a low frequency cross-coupling
of horizontal electric field components with a vertical antenna due to
the aircraft structure.

The Boeing measurement program has provided amplitude data
on the effective heights for a single antenna location on a single
aircraft type. This data is useful in scoping the magnitude of the
above two problems. For the vertical electric field response measured,
the effect of the reflected field from the conducting aircraft surface
was not to enhance the low frequency effective height, but rather to
create aircraft structure resonances in the antenna voltage. This
lack of enhancement in the low frequency effective height, while at
first glance surprising, is not unreasonable when one considers that
the antenna is located near the front of the fuselage and thus the net
reflected field can be appreciably diminished. For the horizontal
electric field response measured, the effect of the aircraft structure
was to provide a low frequency (less than 10 MHz) coupling which was
larger than the vertical coupling by up to a factor of two.

To understand the measurement capability of a particular
electric field antenna on an aircraft, it is necessary to have the com-
plex frequency effective height for the polarizations of interest. In
this regard, the Boeing measurements of the phase were not adequate
because of the ambiguities associated with the data reduction. However,
given the amplitude data as a function of frequency, we have shown
that it is possible to calculate a phase through the use of a causality
constraint on the data. The use of such a calculated complex effective
height for the C-130 aircraft antenna studied has indicated that the
antenna open circuit voltage can be strongly influenced by the horizontal
component of the incident field both in terms of its shape as well as
its amplitude.

The net effect of the contaimination by the horizontal com-
ponent of the incident field is to question the use of blade antennas
on aircraft for electric field measurements where better than a factor
of two or three accuracy is desired. This is particularly important
if frequency domain information over a broad spectrum is wanted.

APPENDIX A.

RELATIONSHIP BETWEEN PHASE AND AMPLITUDE UNDER CAUSALITY CONSTRAINT

There is a relationship between the phase and amplitude of a function in the Fourier domain if we require that the function vanish in the time domain for times less than zero. The constraint that the function vanish for negative times is just causality: i.e., no signal can be detected until it has arrived at the detector. The relationship resulting from this causality constraint is unique for a zero time delay or within a linear phase shift (i.e., ωt) for a given time delay and is known in electric circuit theory as the Bode minimum phase [A-1].

A.1 THEORY

The causality constraint can be expressed mathematically for a function $f(t)$ as:

$$f(t) = 0 \qquad\qquad t < 0$$

$$f(t) = \int_{-\infty}^{\infty} \frac{d\omega}{2\pi}\, e^{-i\omega t}\, \tilde{f}(\omega) \quad t \geqslant 0 \qquad\qquad (17)$$

where the value for $t>0$ is just the inverse Fourier transform. Since the Fourier transform is defined for both positive and negative times, the properties of $\tilde{f}(\omega)$ that allow Eq. 17 to be satisfied are:

1. $\tilde{f}(\omega)$ is analytic in the upper half plane (u.h.p.) of the complex ω plane.

2. $f(\omega) \to o$ uniformly as $|\omega| \to \infty$.

The necessity of these two conditions can be shown by the following:

For $t < o$

$$f(t) = \int_{\infty}^{\infty} \frac{d\omega}{2\pi}\, e^{-i\omega t}\, \tilde{f}(\omega). \qquad\qquad (18)$$

If $\tilde{f}(\omega)$ goes to zero uniformly as $|\omega|$ becomes large, then by using Jordan's Lemma [A-2], we can close the contour in the u.h.p. at $|\omega| \to \infty$ and

$$f(t) = \oint_c \frac{d\omega}{2\pi} e^{-i\omega t} \tilde{f}(\omega) \tag{19}$$

where c is the contour shown in Figure 19.

Now, if $f(\omega)$ is analytic in the u.h.p. [i.e., if all poles and singularities are in the lower half plane (l.h.p.)], then by Cauchy's Theorem A-2], any closed contour integral of an analytic function is zero. Therefore,

$$f(t) = 0$$
$$\text{for } t < 0.$$

A.1.1 Relationship Between Real and Imaginary Parts of an Analytic
       Function

Using these properties of a complex function, $\tilde{f}(\omega)$, we can now derive certain relations between the real and imaginary parts. Let

$$\tilde{f}(\omega) = u(\omega) = i \, v(\omega); \tag{20}$$

then, since $\tilde{f}(\omega)$ is analytic within the contour c of Figure 19, we have from Cauchy's Integral Formula [A-3]:

$$\tilde{f}(\omega) = \frac{1}{2\pi i} \oint_c \frac{dz \, \tilde{f}(z)}{(z-\omega)} . \tag{21}$$

Next, because of the second property of $\tilde{f}(\omega)$, i.e., that it converges uniformly to zero for large ω, we can reduce Eq. 21, to a principal value line integral over the real axis; or

$$\tilde{f}(\omega) = \frac{P}{\pi i} \int_\infty^\infty dz \, \frac{\tilde{f}(z)}{(z-\omega)} . \tag{22}$$

If we now equate the real and imaginary sides of Eq. 22, we have

$$u(\omega) = \frac{P}{\pi} \int_\infty^\infty dz \, \frac{v(z)}{(z-\omega)} \tag{23a}$$
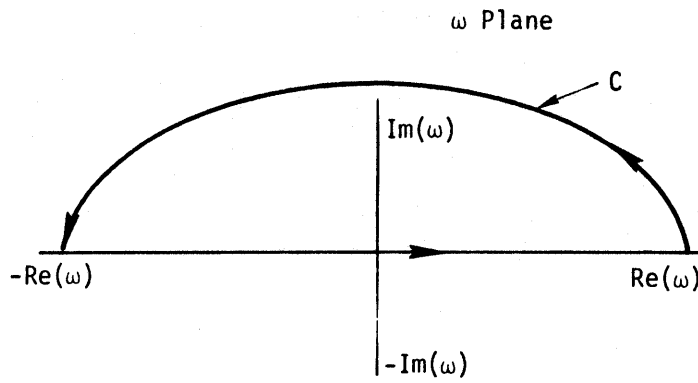
Figure 19. Contour of Integration in Complex ω Plane

$$v(\omega) = \frac{-P}{\pi} \int_\infty^\infty dz \, \frac{u(z)}{(z-\omega)} \quad . \tag{23b}$$

We can further reduce these relations to integrals over half the real axis and eliminate the principal value integral by removing the singularity at $z = \omega$. Noting that

$$P \int_\infty^\infty \frac{dz}{z-\omega} = 0.$$

so that

$$P \int_\infty^\infty \frac{dz}{z-\omega} \, \tilde{f}(\omega) = 0$$

and that

$$u(\omega) = \int_\infty^\infty dt \, \cos(\omega t) \, f(t) = u(-\omega)$$

$$v(\omega) = \int_\infty^\infty dt \, \sin(\omega t) \, f(t) = -v(-\omega)$$

we have

$$u(\omega) = \frac{2}{\pi} \int_0^\infty dz \, \frac{[z \cdot v(z) - \omega \cdot v(\omega)]}{(z^2 - \omega^2)} \tag{24}$$

and

$$v(\omega) = -\frac{2\omega}{\pi} \int_0^\infty dz \, \frac{[u(z) - u(\omega)]}{(z^2 - \omega^2)} \quad . \tag{25}$$

Another useful form for showing the relationship between the real and imaginary parts can be obtained by integrating Eqs. 24 and 25, by parts. Then we have

$$u(\omega) = \frac{1}{\pi\omega} \int_0^\infty dz \, \ln \, \frac{z+\omega}{z-\omega} \, [v(z)-z \, v'(z)] \qquad (26)$$

ανφ

$$v(\omega) = \frac{-1}{\pi} \int_0^\infty dz \, \ln \, \frac{z+\omega}{z-\omega} \cdot u'(z) \qquad (27)$$

As will be noted in Section A.2, by using Equations 24 and 25 or 26 and 27, certain fundamental properties of the real versus imaginary parts can be determined.

A.1.2 Relationship Between Amplitude and Phase for Causal Function

We showed in Section A.1.1 that if $\tilde{f}(\omega)$ was analytic in the u.h.p., then the function $f(t)$ was causal (i.e., $f(t) = 0$ for $t<0$). In addition, we showed that there is a relationship between the real and imaginary parts of $\tilde{f}(\omega)$ when $\tilde{f}(\omega)$ is analytic. We can now make use of this information to derive a relation between the amplitude and phase of such a complex function. Let

$$\tilde{f}(\omega) = u(\omega) + i \, v(\omega) = A(\omega) \, e^{i\phi(\omega)} \qquad (28)$$

where

$$A(\omega) = [u^2 + v^2]^{1/2}$$

$$\phi(\omega) = \tan^{-1} (v/u)$$

or

$$A(\omega) = [f*f]^{1/2}$$

$$\phi(\omega) = \tan^{-1}[(f-f*)/i(f+f*)].$$

We may also define a new function $g(\omega)$ such that

$$\tilde{f}(\omega) = e^{g(\omega)}; \qquad (29)$$

43

thus,

$$g(\omega) = \ln [A(\omega)] + i \phi(\omega). \tag{30}$$

We will now show that $g(\omega)$ has the properties of analyticity and uniform convergence; then we can use the relations between real and imaginary parts to provide the relations between amplitude and phase.

1. Analyticity

If $\tilde{f}(\omega)$ is analytic within a region of the complex ω plane, then $g(\omega)$, equal to $\ln[f(\omega)]$, is analytic except where $|\tilde{f}(\omega)| \to o$.

We can prove this statement by considering the Cauchy-Riemann conditions [A-3] for an analytic function, i.e.,

if

$$\tilde{f}(\omega) = u(\omega) + i\ v(\omega)$$

and

$$\omega = x + iy,$$

then a necessary condition for analyticity of $\tilde{f}(\omega)$ is

$$\frac{\partial u}{\partial x} = \frac{\partial v}{\partial y} \quad \text{and} \quad \frac{\partial u}{\partial y} = \frac{-\partial v}{\partial x} \tag{31}$$

and a sufficient condition is that the derivatives are continuous.

Let $\qquad g(\omega) = R(\omega) + i\ I(\omega).$

Then, $\qquad u(\omega) = e^{R(\omega)} \cos [I(\omega)]$

and $\qquad v(\omega) = e^{R(\omega)} \sin [I(\omega)].$

Now, if $\tilde{f}(\omega)$ is analytic, then we have

$$\frac{\partial}{\partial x} \left[e^{R(\omega)} \cos I(\omega) \right] = \frac{-\partial}{\partial y} \left[e^{R(\omega)} \sin I(\omega) \right] \tag{32}$$

and

$$\frac{\partial}{\partial y}\left[e^{R(\omega)}\cos I(\omega)\right] = \frac{-\partial}{\partial x}\left[e^{R(\omega)}\sin I(\omega)\right] \; . \tag{32}$$

Therefore, after manipulating these two equations we have

$$e^{R(\omega)}\;\frac{\partial R(\omega)}{\partial x} - \frac{\partial I(\omega)}{\partial y} = 0$$

$$\tag{33}$$

$$e^{R(\omega)}\;\frac{\partial R(\omega)}{\partial y} + \frac{\partial I(\omega)}{\partial x} = 0 \; .$$

As long as $R(\omega) > -\infty$, the Cauchy-Rieman, conditions are met and the derviatives of R and I are continuous since $A(\omega)$ and $\phi(\omega)$ have no discontinuities. Thus, $g(\omega)$ is analytic within the region that $\tilde{f}(\omega)$ is analytic. However, as $|\omega|\to\infty$, $\tilde{f}(\omega)\to 0$ and $\ln[\tilde{f}(\omega)]\to -\infty$, so $g(\omega)$ has a singularity at $|\omega| = \infty$.

We can transform this singularity at ∞ to one at the orgin if we know how $\tilde{f}(\omega)\to 0$ as $\omega\to\infty$.

If $\qquad\qquad \tilde{f}(\omega)\to 0 \quad$ as $\quad \tilde{f}_\infty(\omega) = A_\infty(\omega)\;e^{i\phi_\infty} \; ,$

$$|\omega|\to\infty$$

then we can create a new function $h(\omega)$ where

$$h(\omega) = g(\omega) - \ln[\tilde{f}_\infty(\omega)] = \ln[A(\omega)/A_\infty(\omega)]+i(\phi-\phi_\infty) \; . \tag{34}$$

Now, if $\tilde{f}_\infty(\omega)$ is analytic in the u.h.p. except for simple poles on the real axis (which we can handle by principal value integrals), then $h(\omega)$ has the properties that it is analytic in the u.h.p. with only logarithmic singularities on the real axis and converges to zero uniformly as $|\omega|\to\infty$. This new function can be used to relate the amplitude and phase with Equations 24 and 25 as:

$$\ln\left[A(\omega)/A_\infty(\omega)\right] = \frac{2}{\pi}\int_0^\infty dz \frac{\{z[\phi(z)-\phi_\infty(z)]-\omega[\phi(\omega)-\phi_\infty(\omega)]\}}{(z^2-\omega^2)} \tag{35}$$

45

and

$$\left[\phi(\omega) - \phi_\infty(\omega)\right] = \frac{2\omega}{\pi} \int_0^\infty dz \, \frac{\left\{\ln[A(z)/A_\infty(z)] - \ln[A(\omega)/A_\infty(\omega)]\right\}}{(z^2 - \omega^2)} \tag{36}$$

A.2   APPLICATION OF CAUSAL PHASE AND AMPLITUDE RELATIONSHIP

The principal uses of Eq. 34 and 35 in this report are to check and correct the phase and amplitude data over a frequency regime $\omega_0 < \omega < \omega_1$ and to provide a basis for extrapolating that data without generating any causal errors in the transform. In this regard, it is important to note a few trends in the relations between phase and amplitude.

A.2.1   Constant Amplitude

When $A(\omega)$ is constant for $0 < \omega < \omega_0$, then from Eq. 35, we see that the phase will increase linearly from zero. This can be shown as follows:

$$A(\omega) = A_0 \quad \omega < \omega_0.$$

Then Equation 36 becomes

$$\phi(\omega) - \phi_\infty = \frac{-2\omega}{\pi} \left\{ \int_0^{\omega_0} dz \, \frac{\ln[A_\infty(\omega)/A_\infty(z)]}{(z^2-\omega^2)} \right.$$

$$\omega < \omega_0$$

$$\left. + \int_{\omega_0}^\infty dz \, \frac{\ln([A(z) \cdot A_\infty(\omega)]/[A_0 \cdot A_\infty(z)])}{(z^2-\omega^2)} \right\} \tag{37}$$

or

$$\phi(\omega) = \left\{ \phi_\infty - \frac{2\omega}{\pi} \int_0^\infty dz \, \frac{\ln[A_\infty(\omega)/A_\infty(z)]}{(z^2-\omega^2)} \right\} - \frac{2\omega}{\pi} \int_0^\infty dz \, \frac{\ln[A(z)/A_0]}{(z^2-\omega^2)} \tag{38}$$

$$\omega < \omega_0$$

but

$$\phi_\infty = \frac{2\omega}{\pi} \int_0^\infty \frac{dz}{(z^2-\omega^2)} \, \ln[A_\infty(\omega)/A_\infty(z)]. \tag{39}$$

46

Therefore,

$$\phi(\omega) = \frac{-2\omega}{\pi} \int_{\omega_0}^{\infty} dz \; \frac{\ln[A(z)/A_0]}{(z^2-\omega^2)} \qquad (40)$$
$$\omega < \omega_0$$

or since $\omega < \omega_0 \leq z$

$$\boxed{\phi(\omega) \simeq \omega \cdot \left\{ \frac{-2}{\pi} \int_{\omega_0}^{\infty} \frac{dz}{z^2} \; \ln[A(z)/A_0] \right\}} \qquad (41)$$
$$\omega < \omega_0$$

Thus, if we have a constant amplitude, the phase will rise linearly with ω as shown in Figure 20.

A.2.2 Amplitude Falloff

If $A(\omega)$ goes to zero like $1/\omega^m$, then the phase shift at $\omega = \infty$ can be determined to be $m \frac{\pi}{2}$. To show this, we look at the relation

$$\phi_{\infty} = \frac{-2\omega}{\pi} \int_{0}^{\infty} dz \; \frac{\ln[\omega^m/z^m]}{(z^2-\omega^2)}, \qquad (42)$$

or

$$\phi_{\infty} = \left(\frac{2\omega}{\pi}\right)^{(m)} \int_{0}^{\infty} \frac{dz}{\omega^2} \; \frac{\ln[z/\omega]}{(z^2/\omega^2-1)}. \qquad (43)$$

Let $u = z/\omega$.

Then

$$\phi_{\infty} = \frac{2m}{\pi} \left\{ \int_{0}^{1} du \; \frac{\ln(u)}{(u^2-1)} + \int_{1}^{\infty} du \; \frac{\ln(u)}{(u^2-1)} \right\} \qquad (44)$$

or

$$\phi_{\infty} = \frac{4m}{\pi} \int_{0}^{1} du \; \frac{\ln(u)}{(u^2-1)} \qquad . \qquad (45)$$

Therefore,

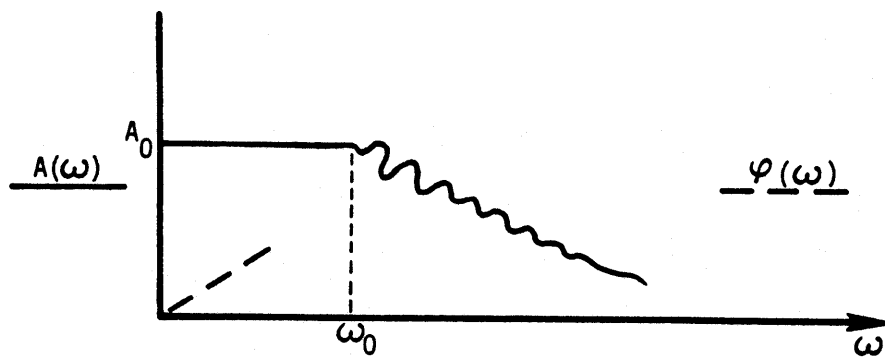$$\phi_{\infty} = \frac{4m}{\pi} \left(\frac{\pi^2}{8}\right) \qquad (46)$$

47

Figure 20.   Phase for a Constant Amplitude

or

$$\boxed{\phi_\infty = m \frac{\pi}{2}} \tag{47}$$

To understand how the phase approaches this value, ϕ_∞, we can look at the value of $\phi(\omega)$ when ω becomes large. When $A(\omega) \simeq A_\infty(\omega)$ for $\omega > \omega_1$ Equation 35 becomes

$$\phi(\omega) - \phi_\infty(\omega) \simeq - \frac{2\omega}{\pi} \int_0^{\omega_1} dz \frac{\ln A(z)/A_\infty(z)}{(z^2 - \omega^2)} \tag{48}$$

or

$$\phi(\omega) \simeq \phi_\infty + \frac{1}{\omega} \cdot \left\{ \frac{2}{\pi} \int_0^{\omega_1} dz \ln[A(z)/A_\infty(z)] \right\} . \tag{49}$$

Thus, $\phi(\omega) \to \phi_\infty$ like $1/\omega$ and approaches from above or below depending on whether $A(z)$ is greater than or less than $A_\infty(z)$ over the range of integration. Figure 21 shows this trend.

A.2.3 Phase in Region of Amplitude Variation

To help understand the variation in phase for rapid amplitude variations, we can look at Equation 24 and 25 for different conditions.

First, let us consider the case where the phase varies from $\pm\pi$ to 0 as shown in Figure 21a.

$$\text{Case 1:} \quad \phi(\omega) = \pi \cdot U(\omega_0 - \omega)$$

$$\phi'(\omega) = -\pi \delta(\omega_0 - \omega)$$

Using Equation 24, where $v(\omega) = [\phi(\omega) - \phi_\infty(\omega)]$ and $u(\omega) = \ln[A(\omega)/A_\infty(\omega)]$, we have

$$\ln[A(\omega)/A_\infty(\omega)] = \frac{1}{\pi\omega} \int_0^\infty dz \ln \left| \frac{z+\omega}{z-\omega} \right| [\pi U(\omega_0 - z) - z\pi \delta(\omega_0 - z)] . \tag{50}$$

Therefore,

$$\ln[A(\omega)/A_\infty(\omega)] = \frac{1}{\omega} \left\{ \int_0^{\omega_0} dz \ln \left| \frac{z+\omega}{z-\omega} \right| - \omega_0 \ln \left| \frac{\omega_0 + \omega}{\omega_0 - \omega} \right| \right\} \tag{51}$$

$$= \frac{1}{\omega} \left\{ \omega \ln \left| \omega_0^2 - \omega^2 \right| - \omega \ln \omega^2 \right\}$$

49

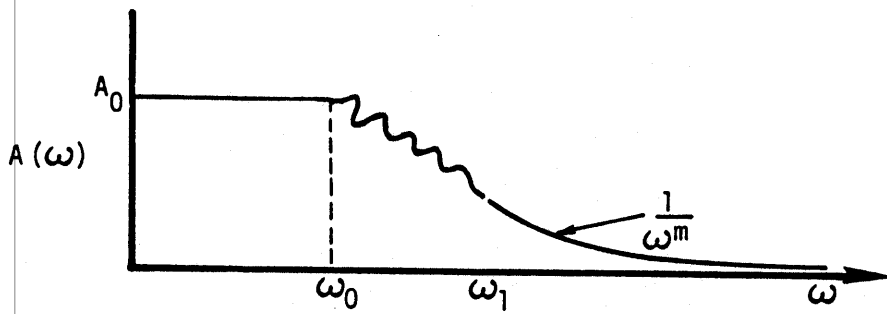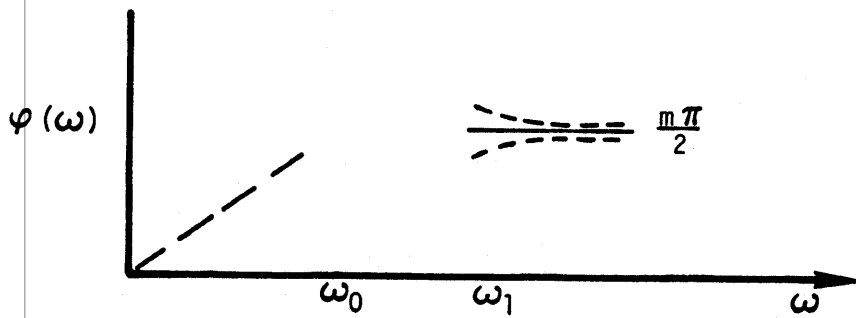Figure 21a. Amplitude Function
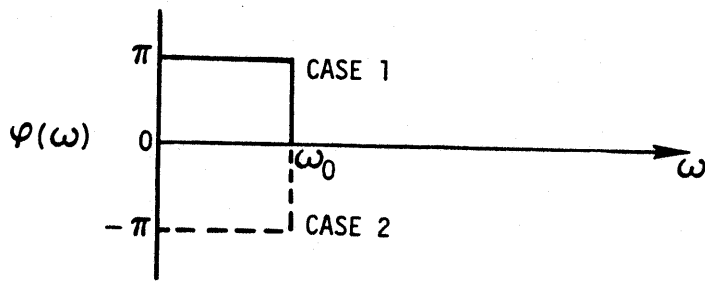

Figure 21b.   Phase Function
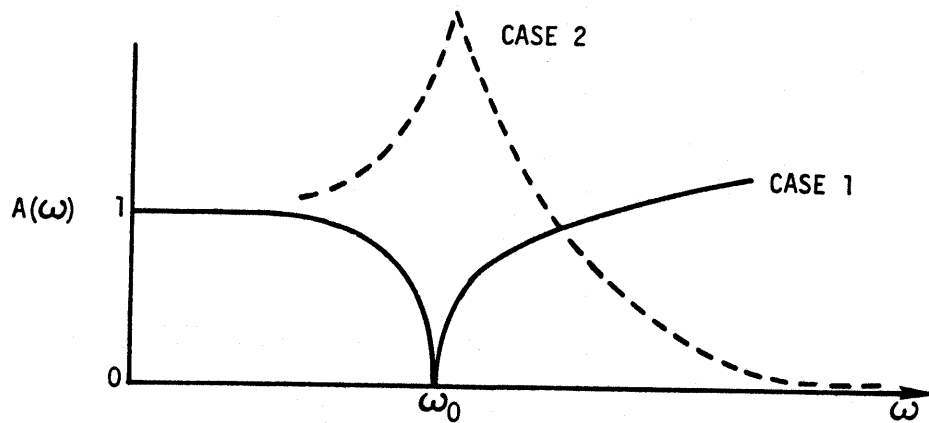
50

Figure 22a. π Shift in Phase

Figure 22b. Amplitude for π Shift in Phase

51

or

$$\ln A(\omega)/A_\infty(\omega) = \ln \left| \frac{\omega_0{}^2 - \omega^2}{\omega^2} \right| . \tag{52}$$

Thus,

$$A(\omega) = \left| \frac{\omega_0{}^2 - \omega^2}{\omega_0{}^2} \right| \tag{53}$$

$$A_\infty(\omega) = \frac{\omega^2}{\omega_0{}^2} .$$

Figure 22b shows this form. Thus for a phase shift from $+\pi$ to 0, the amplitude goes through a null.

$$\text{Case 2:} \quad \phi(\omega) = -\pi \, u(\omega_0 - \omega)$$

$$\phi'(\omega) = \pi \delta(\omega_0 - \omega)$$

For this case we note that Equation 24 becomes

$$\ln [A(\omega)/A_\infty(\omega)] = \frac{1}{\pi} \left\{ -\int dz \ln \left| \frac{z+\omega}{z-\omega} \right| + \omega_0 \ln \left| \frac{\omega_0+\omega}{\omega_0-\omega} \right| \right\}$$

$$= \ln \left| \frac{\omega^2}{\omega_0{}^2 - \omega^2} \right| \tag{54}$$

Therefore,

$$A(\omega) = \frac{\omega_0{}^2}{|\omega_0{}^2 - \omega^2|} \tag{55}$$

$$A_\infty(\omega) = \frac{\omega_0{}^2}{\omega^2}$$

Thus for a π shift in phase with a positive slope, the amplitude goes through a resonance as shown in Figure 22b.

REFERENCES

A-1. H. W. Bode, Network Analysis and Feedback Amplifier Design, D.
      Van Nostrand Company, Inc., Princeton, New Jersey, 1945.

A-2. E. T. Wittaker and G. N. Watson, A Course of Modern Analysis,
      Cambridge University Press, London, England, 1963.

A-3. P. M. Morse and H. Feshback, Methods of Theoretical Physics, McGraw-
      Hill Book Company, Inc., New York, New York.

APPENDIX B

DIFFICULTIES IN USING THE MEASURED EFFECTIVE HEIGHT DATA

Difficulties were encountered in using the Boeing effective height data to study the effect of the aircraft response on the measuring of vertical electric fields. The major difficulty was in the lack of a causal relationship between the phase and the amplitude functions. This lack of causality is believed to be due to the ambiguity in the phase data reduction and in misinterpretation of the original lack of agreement between the 45° data and the vertical and horizontal data.

B.1 CORRELATION OF 45° DATA WITH THE VERTICAL AND HORIZONTAL DATA

The Boeing measurement program on the effective height of a 1-m blade antenna on a C-130 aircraft produced amplitude and phase data for three polarizations: vertical, horizontal and at 45° (Ref. B-1). Figure 23 shows the orientation of these polarizations relative to the aircraft and the antenna. The estimates of the errors in these measurements were ±2 dB for the amplitude and ±30° for the phase. As part of a review for DNA on the preliminary draft (Ref. B-3) of the measurement results, we noted that the horizontal and vertical data did not correlate with the 45° data. Based on our comments, Boeing reviewed their data and concluded that because of the ±180° ambiguity in the phase measurements, a ±n90° ambiguity resulted in their data reduction scheme between different scaled bands of the frequency region measured (Ref. B-2). Thus they changed the phase within certain scaled frequency bands of the data to bring the three polarizations into correlation. Figure 24 shows the scaled frequency bands used in the 0.5 to 100 MHz regions. We now believe that this change in the phase has resulted in a non-causal relationship between phase and amplitude.

In terms of our original comments on the non-correlation of the 45° data, we believe the major problem was in defining a consistent definition of positive and negative measurements. Referring to Figure 23, we note that if a field polarized like E_V is assumed to produce a positive signal from the antenna (V_V), then a field polarized like E_H will produce a negative signal (V_H). This can be easily seen in the limit of a low frequency quasi-static field. For a horizontal field pointed toward the tail, the electrons on the fuselage surface will move toward the front or cockpit creating a negative radial electric field near the antenna. Therefore, a field polarized like E_{45} in Figure 23
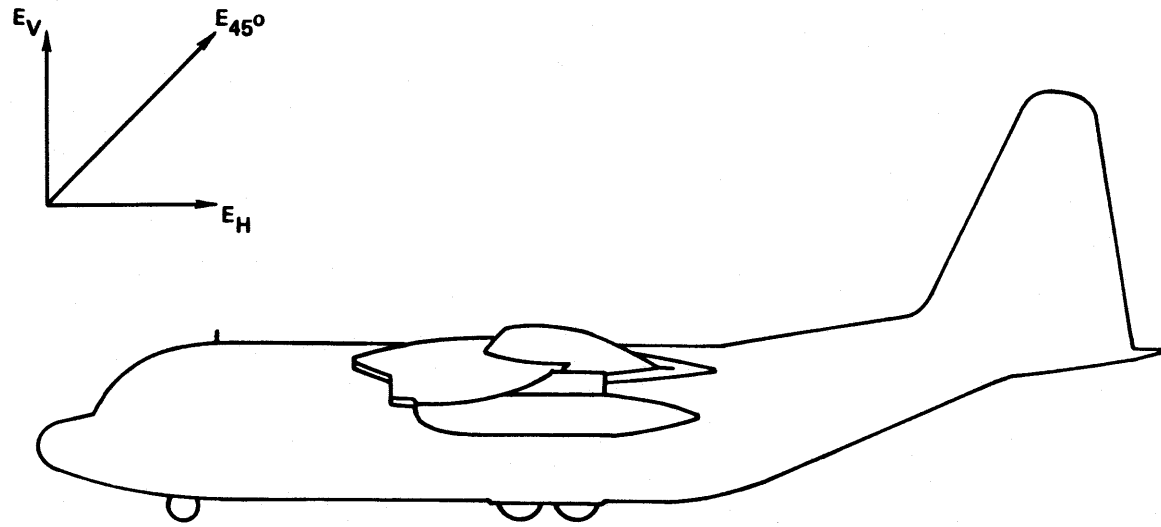
55

Figure 23. Orientation for Free Field Relative to the C-130 Model Aircraft

1/200 SCALE

1/72 SCALE

1/20 SCALE
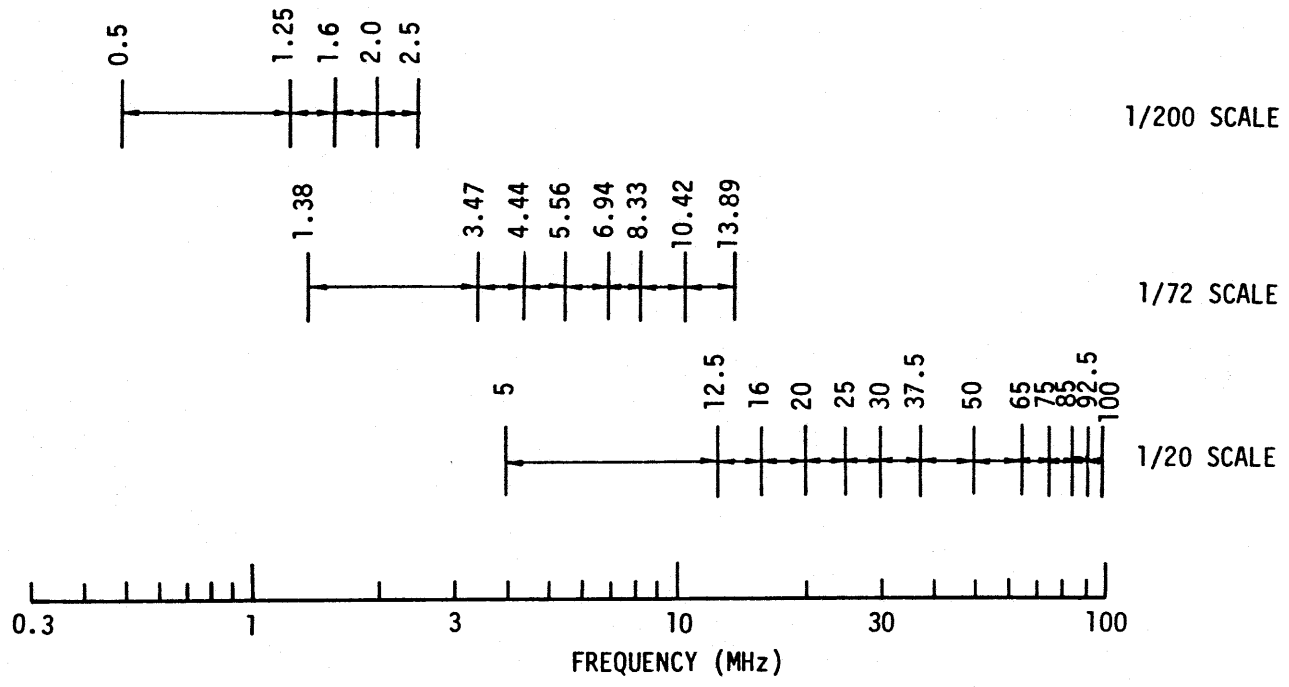
0.3 1 3 10 30 100

FREQUENCY (MHz)

Figure 24. Scaled Frequency Bands

would produce canceling signals at the antenna and the V_{45} signal would be the difference between the V_H and V_V signals for low frequency or

$$V_{45} = |V_V| - |V_H|. \qquad (56)$$

Figure 25 shows an overlay of the three sets of amplitude data measured by Boeing. On the graph we can see that $|V_H| \geq |V_V|$ for frequencies below 7 MHz and that at 4 MHz the amplitude are equal which would account for the null seen in the V_{45} data. Thus the phase for the 45° data should have started at -180°, increased toward 0° near 7 MHz with a dip in the phase at 4 MHz to account for the nulling of the amplitude, as indicated by the relationship of phase and amplitude discussed in Appendix A. Figures 26 through 28 show the low frequency phase data presented by Boeing both in their preliminary draft (Ref. 3) and the final report (Ref. 1). As can be seen, the horizontal phase data was kept constant but both the vertical and 45° data changed. Note in Figure 27 that the vertical data below 4 MHz was shifted by 180° to account for the lack of correlation between the three polarizations. As was discussed above, this shift of 180° should have been attributed to the 45° data. In addition to this major change in the vertical data, there were also other changes made at higher frequencies. The point to be made is that the phase data as reported has considerable ambiguities which put in questionits accuracy to ±30°.

In the next two sections, we discuss our calculations which show that the effective height data is non-causal and the effect of that condition on the resulting open circuit voltage calculations. In Section B.4, using the measured amplitude data and the calculated phase functions discussed in the text, we present the calculated 45° amplitude and phase for comparison with the measured 45° data.

B.2 VERTICAL DATA CAUSALITY

As was noted above, the measurements of effective height phase and amplitude do not appear to be causal. To show this lack of causality, the frequency data was transformed to the time domain to observe the delta function response. The procedure for calculating this transform was as follows. First, the vertical data was extrapolated beyond the range of measurements to prevent the introduction of spurious signals in the time domain for sharp cut-offs in the frequency domain. For
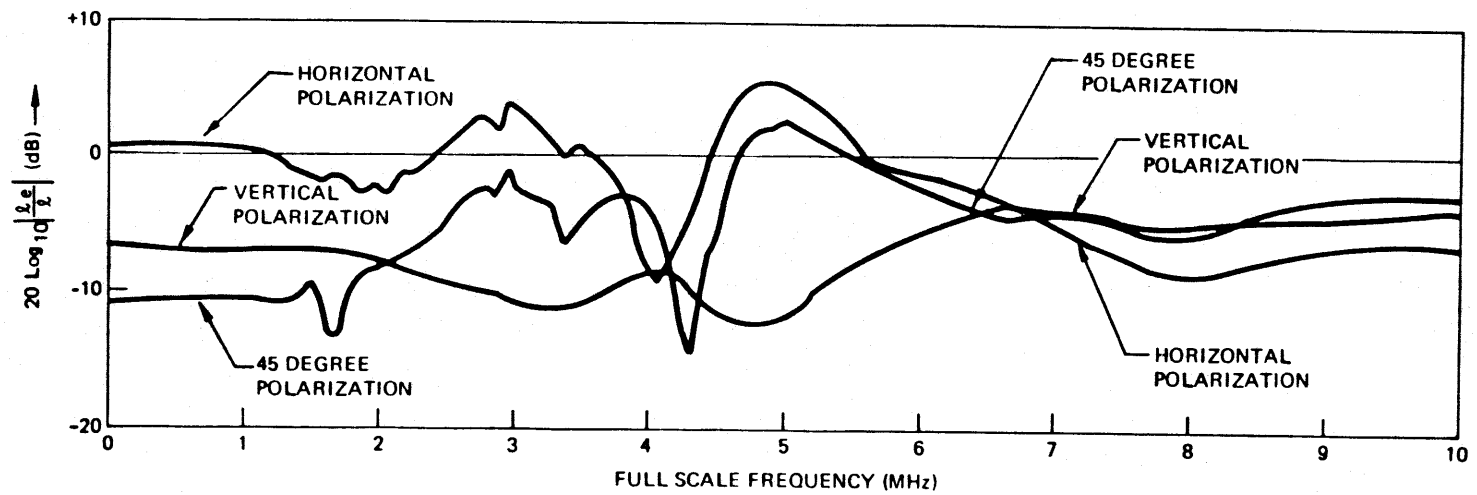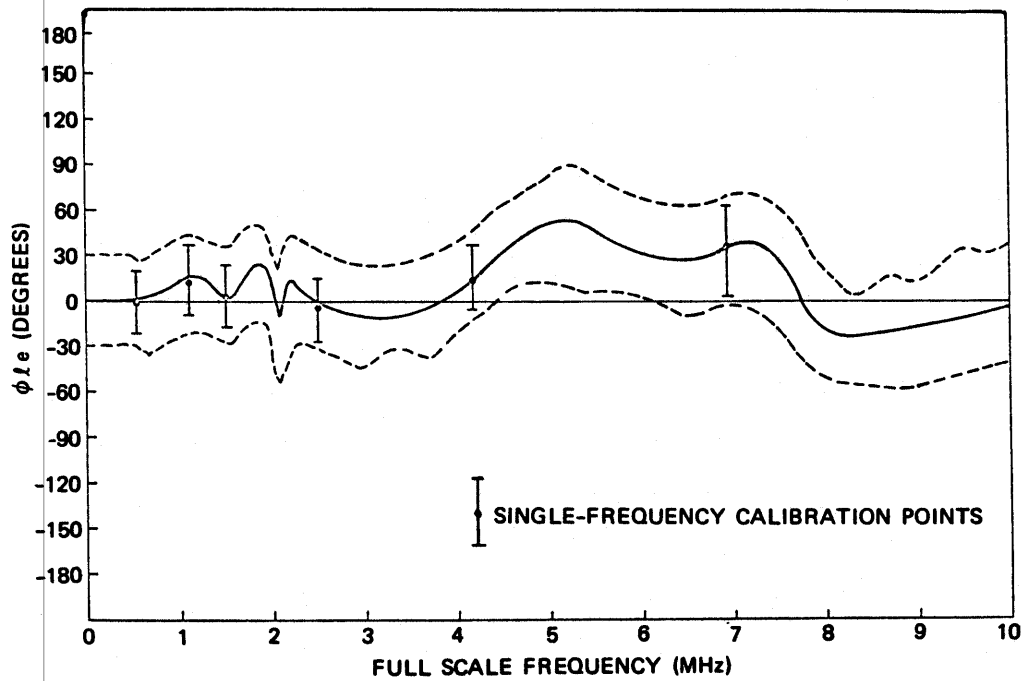
Figure 25.   Effective Length Amplitude

Figure 26a. Effective Length Phase Horizontal
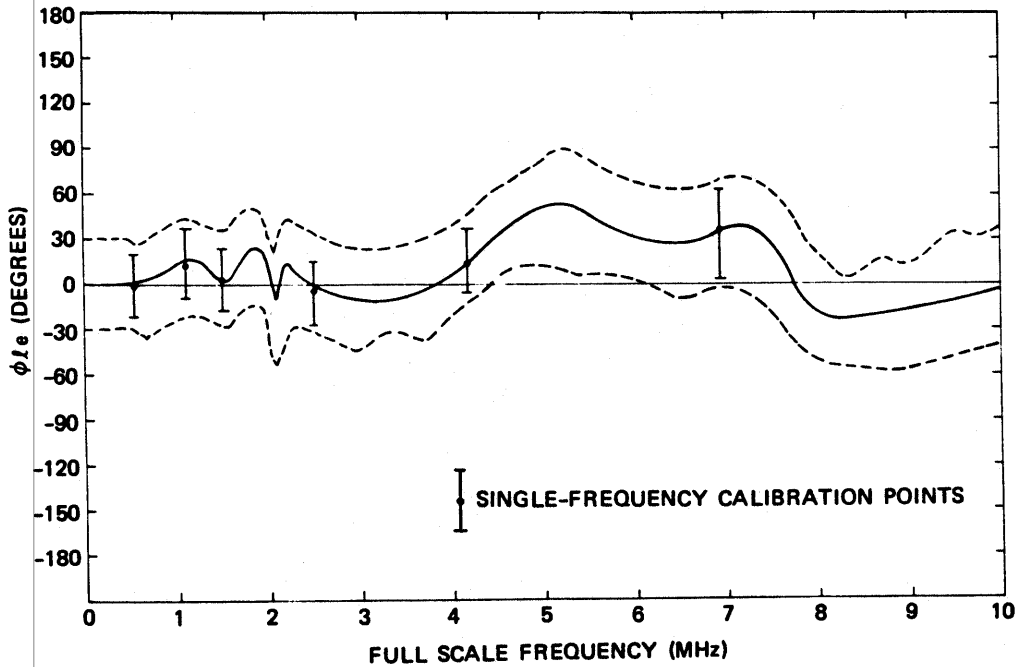Polarization (Preliminary)

Figure 26 b. Effective Length Phase Horizontal
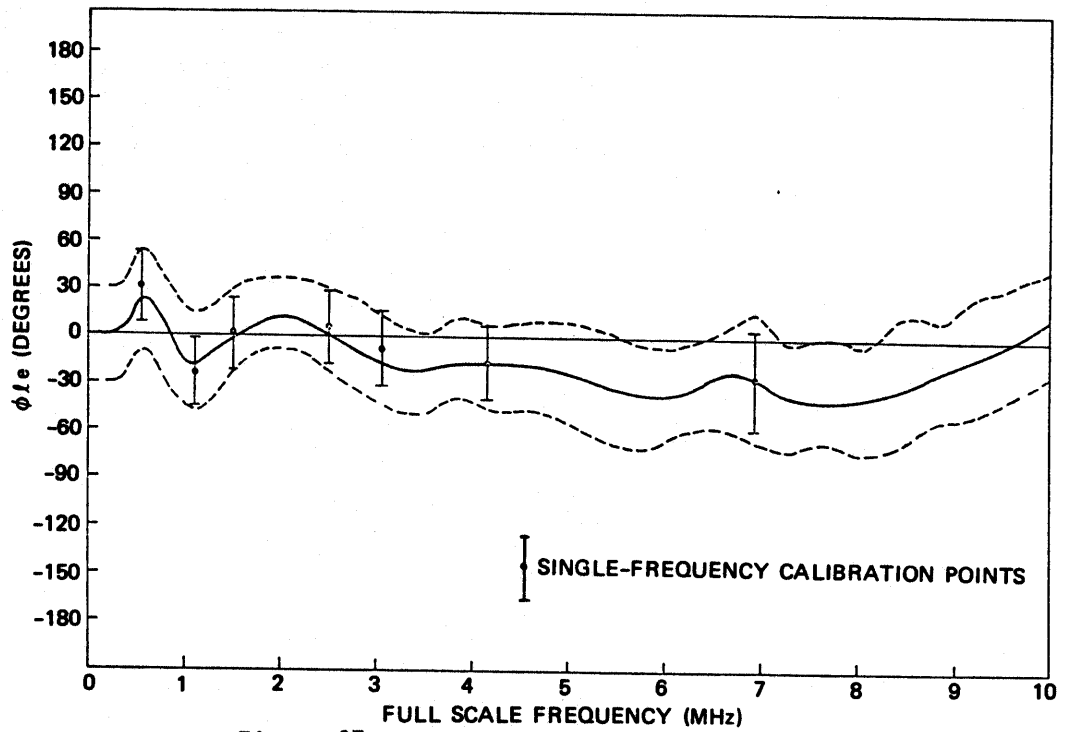Polarization (Final)

60

Figure 27a. Effective Length Phase Vertical
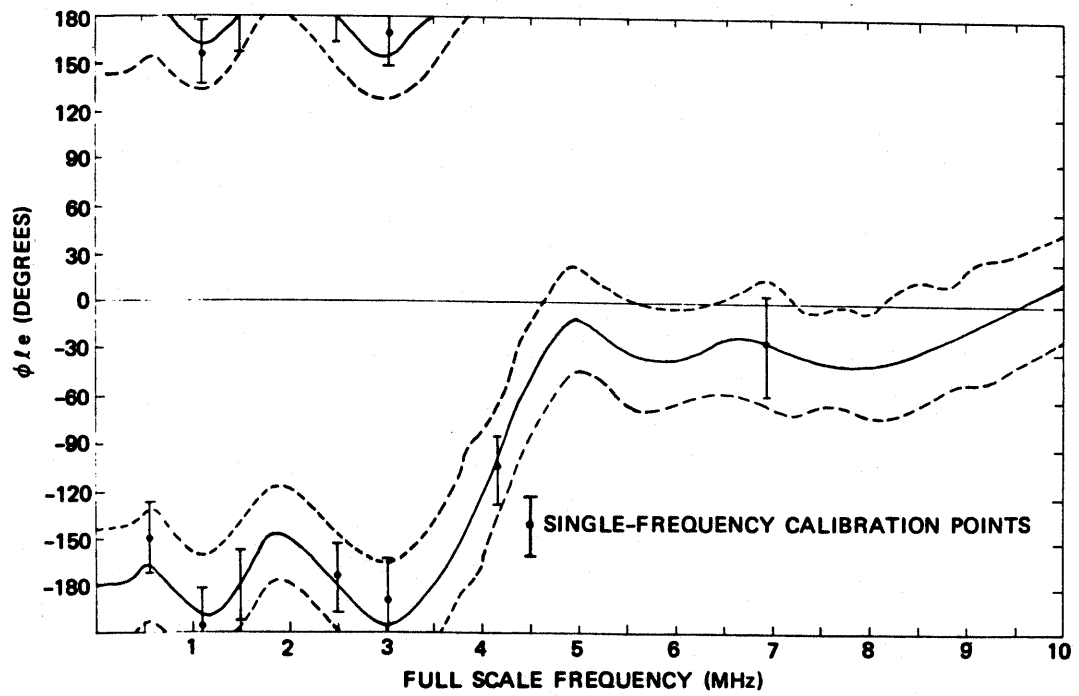Polarization (Preliminary)

Figure 27 b. Effective Length Phase Vertical
Polarization (Final)
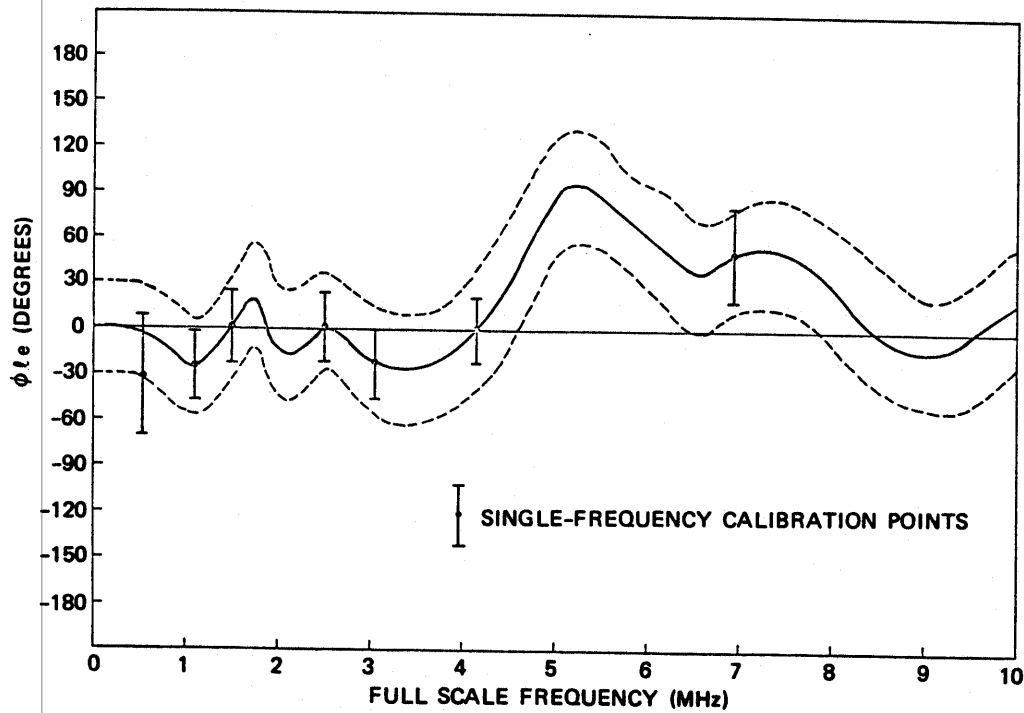
Figure 28a.   Effective Length 45 Degree
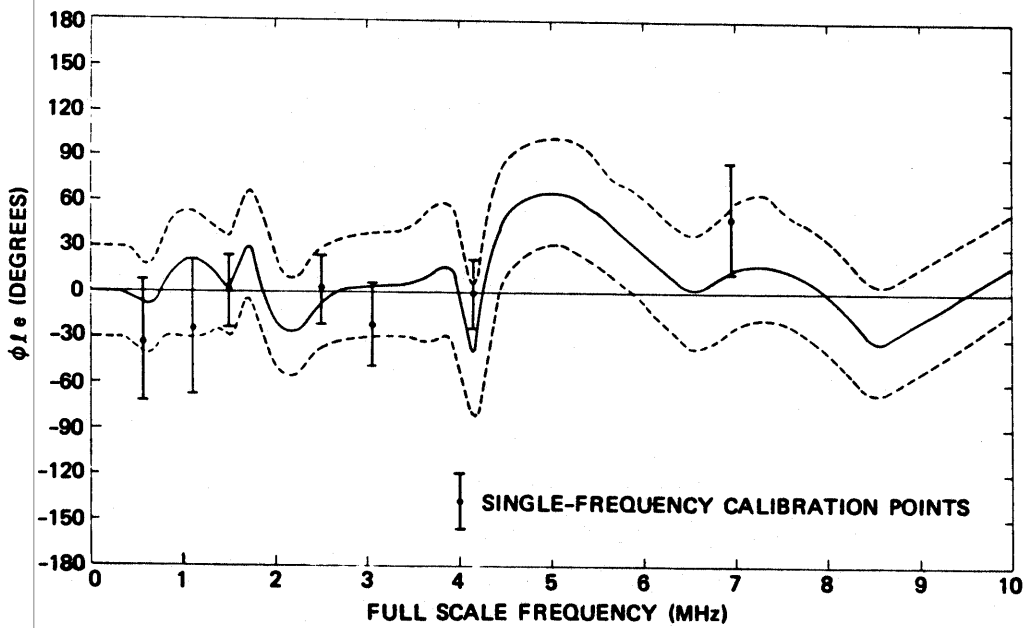   Polarization (Preliminary)

Figure 28b.   Effective Length 45 Degree
          Polarization (Final)

frequencies below 0.5 MHz the amplitude was assumed constant and the phase varied linearly to $-\pi$. For frequencies above 100 MHz, the amplitude was fit by the function discussed in Section II while the phase was extrapolated by the function

$$\phi(\omega < 2\pi \cdot 100 \text{ MHz}) = \tan^{-1}\left(\frac{\omega^2 - \omega_o^2}{\omega \Delta \omega}\right) \tag{57}$$

which corresponds to phase for an amplitude resonance of the form in Equation 10. The transform equation was

$$h_e(t) = \int_{\omega_N}^{\omega_N} \frac{d\omega}{2\pi} e^{-i\omega t} A(\omega) e^{i\phi(\omega)} \tag{58}$$

and was solved numerically by an FFT subroutine for ω_N equal to $2\pi \cdot 2 \text{GHz}$. Figure 29 shows the resulting hime history of h_e. The negative time values were obtained by changing the sign in the exponent of Eq. 58 from $-$ to $+$. Note the rather large precursor that results, which can significantly alter the calculation of an open circuit voltage. Also shown in Figure 29 is the delta function response for the amplitude data combined with the calculated phase function discussed in Section II. While there is still a precursor evident, its magnitude is less and its damps out quicker. As an example of the effect of this precursor on the open circuit voltage calculation, Figure 30 shows a voltage calculation of the Case 2 waveform discussed in Section III for both the reported vertical effective height and the amplitude combined with a calculated phase.

B.3   HORIZONTAL DATA

A calculation similar to the one discussed in Section B.2 was performed to look at the causality relationship of the horizontal data. Figure 31 shows the delta function response for the amplitude and phase reported versus a function utilizing the amplitude data with the causal phase function discussed in Section II. The calculation was performed using an FFT substantive to solve Equation 58, where the extrapolated values of the data were as follows. First, for frequencies below 0.5 MHz, the amplitude data was considered constant and the phase taken linearly to zero at $\omega = o$. Second, for frequencies above 100 MHz, the amplitude was fit by the function given in Equation 12, which provided
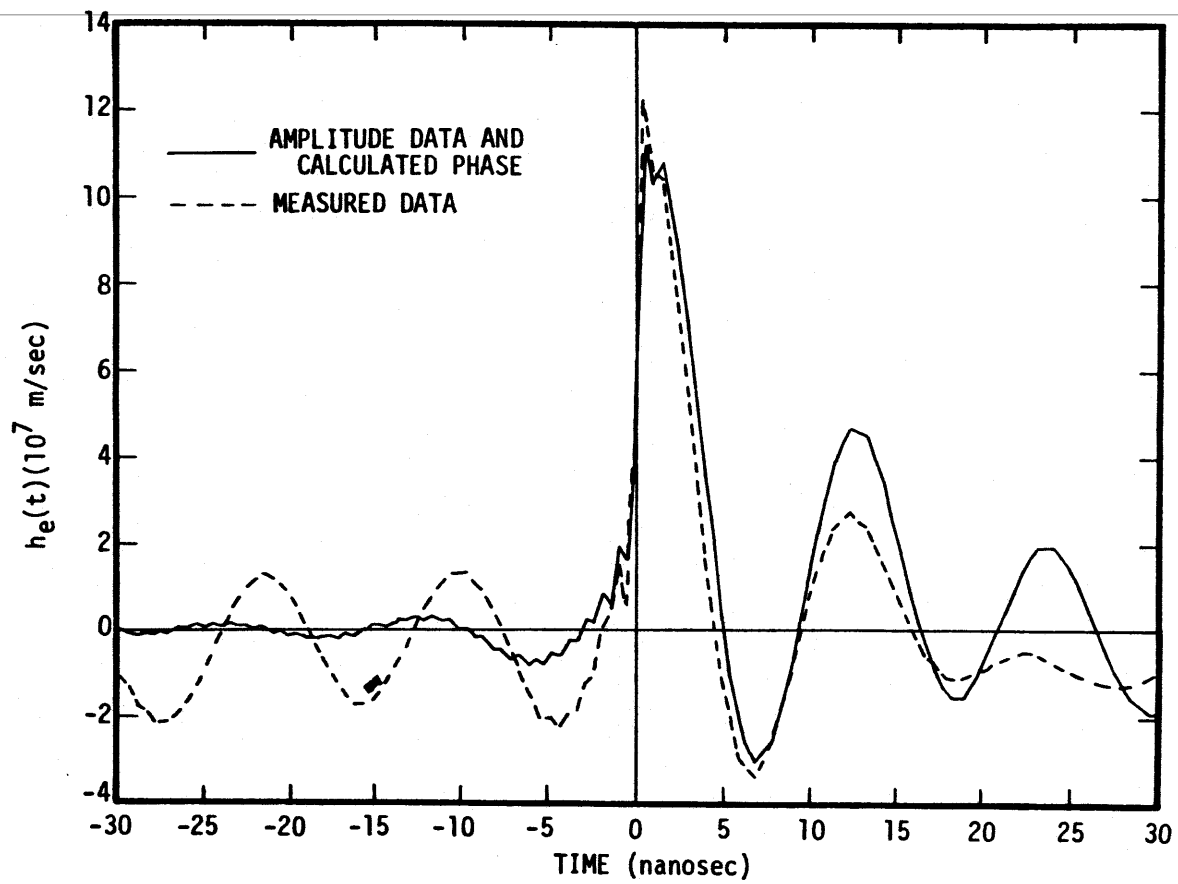
63

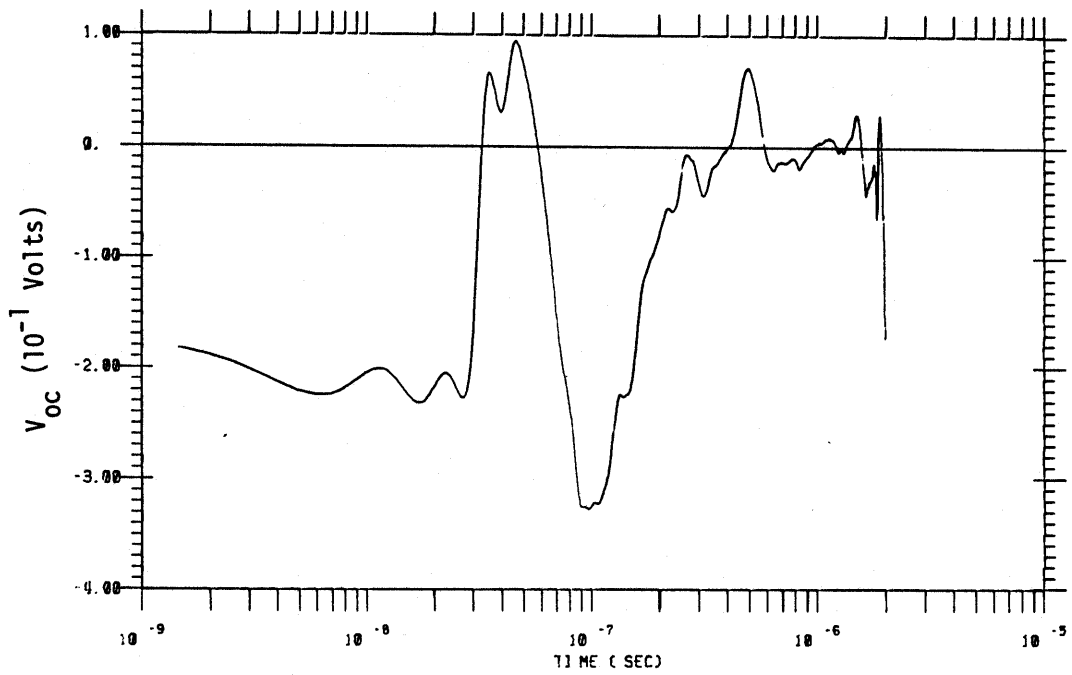Figure 29. Vertical Polarization $h_e(t)$

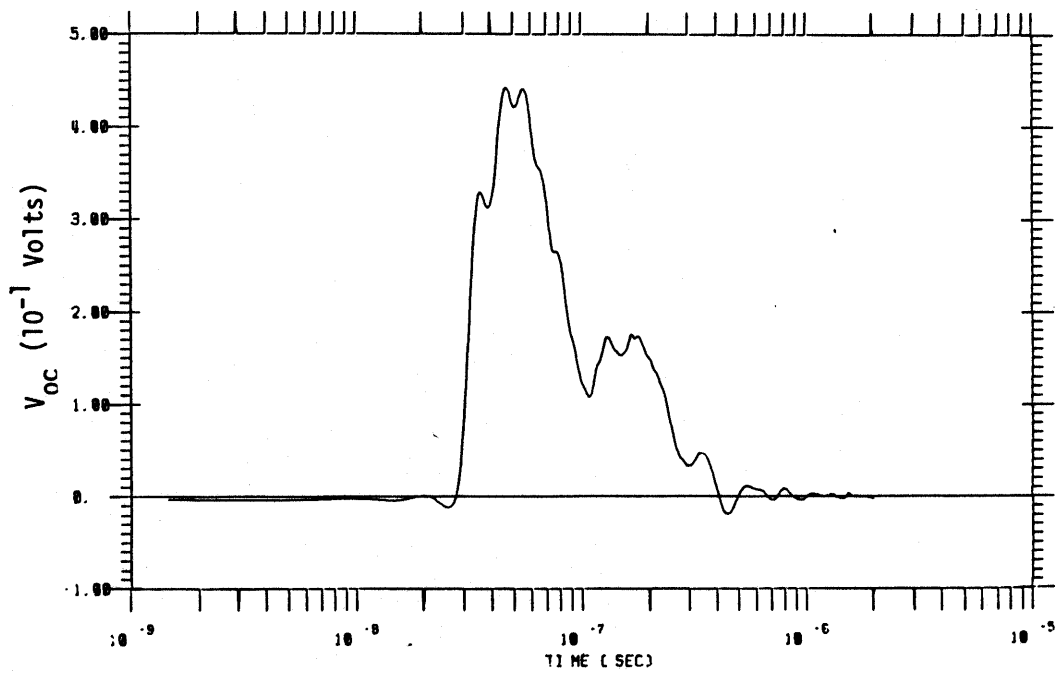Figure 30a. V_{oc} for Measured Effective Height (Vertical Polarization)

Figure 30b. V_{oc} for Measured Amplitude and Calculated Phase
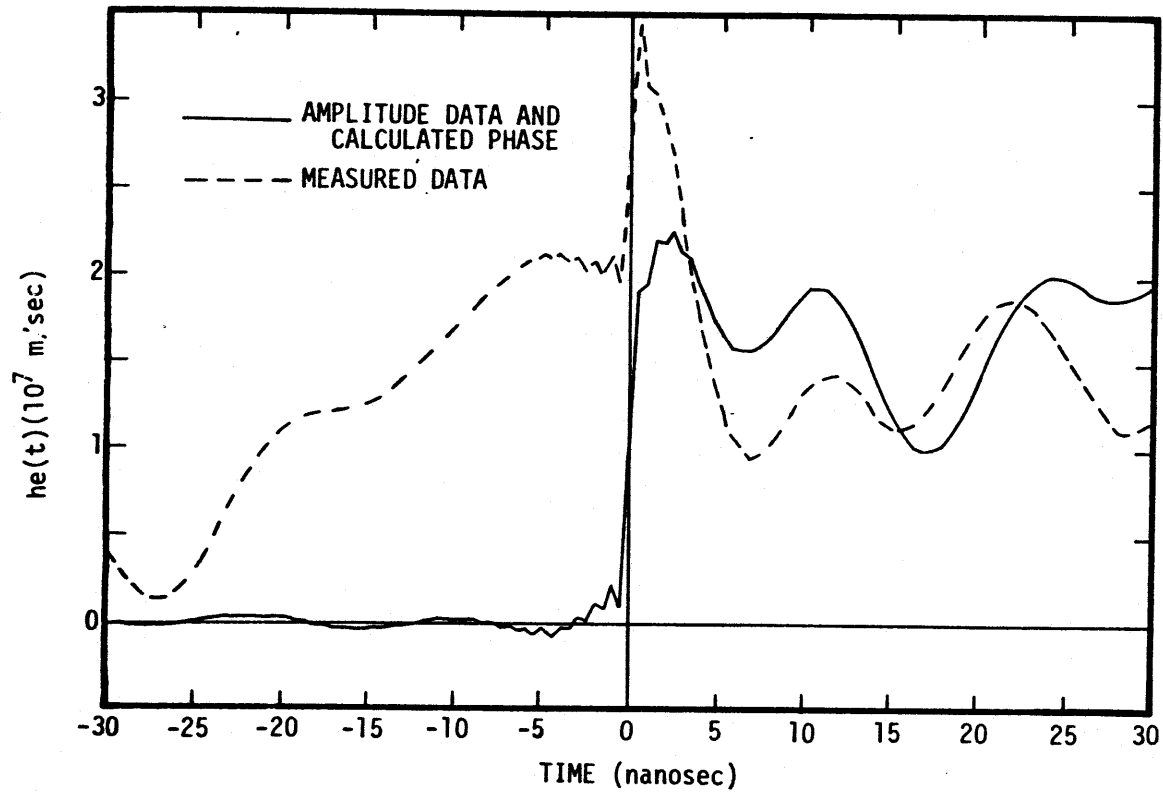(Vertical Polarization)

65

Figure 31. Horizontal Polarization $h_e(t)$

a smooth transition to a $1/\omega$ decay and the phase was extrapolated by

$$\phi(\omega < 2\pi \cdot 100 \text{ MHz}) = \tan^{-1} \omega/\omega_0 \qquad (59)$$

where $\qquad \omega_0 = 2\pi \cdot 2 \text{ MHz}.$

The delta function response curve for the amplitude data and calculated phase function was calculated in the same manner.

Again, as an example of the effect of this precursor, calculations of the open circuit voltage were made using the measured phase and the calculated causal phase function. Figure 32 shows the results for an incident field of the form shown in Section III for Case 2.

Note in this case that although the precursor was larger, its effect was not as dramatic as for the vertical polarization, but its effect was still significant.

B.4 45° CALCULATION

As a further check on the accuracy of the antenna effective heights generated from the amplitude data and the causal relationship between phase and amplitude, we have combined the horizontal and vertical effective heights to compare with the measured 45° data. Using the orientation shown in Figure 23 and our definition of E_V producing a positive antenna output voltage, we have combined the effective heights in the following manner:

$$|h_{45}| = \left[|h_v|^2 + |h_h|^2 - 2h_v h_h \cos(\phi_v - \phi_h) \right]^{1/2} \cdot \cos(45) \qquad (60)$$

and $\qquad \phi_{45} = \tan^{-1} \left\{ \dfrac{|h_v|\sin\phi_v - |h_h|\sin\phi_h}{|h_v|\cos\phi_v - |h_h|\cos\phi_h} \right\} \qquad (61)$

Figure 33 shows the amplitude calculated from Equation 60. Figure 24 shows the phase from Equation 61. Also shown in Figure 33 is the error bound of the measured 45° amplitude data. At first glance, the comparison appears to be fairly good particuarly in terms of the
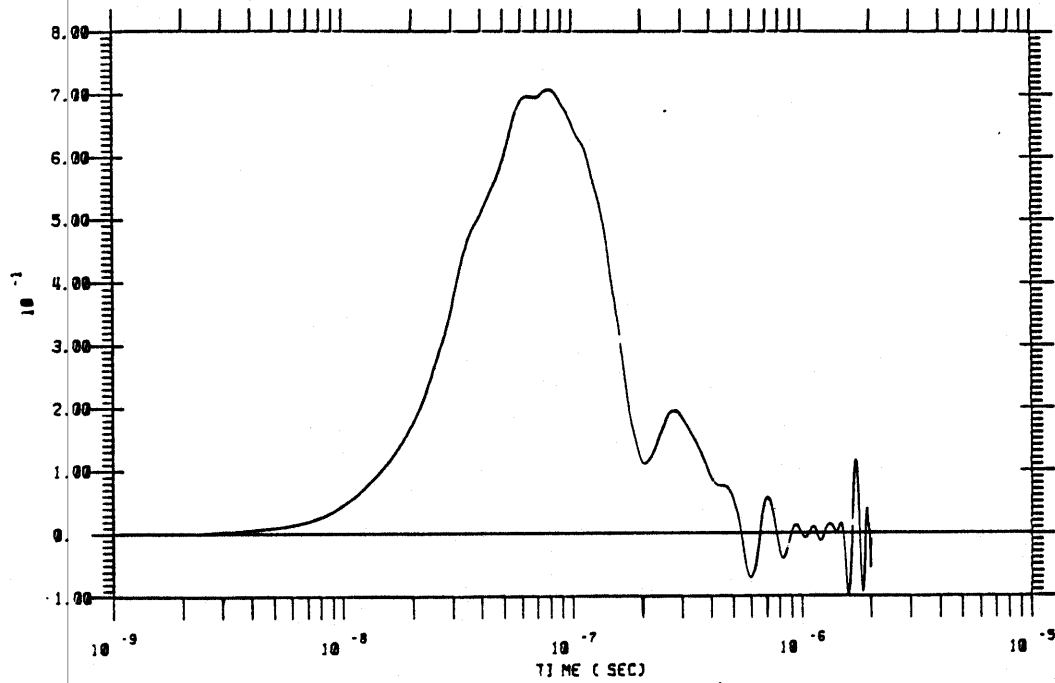
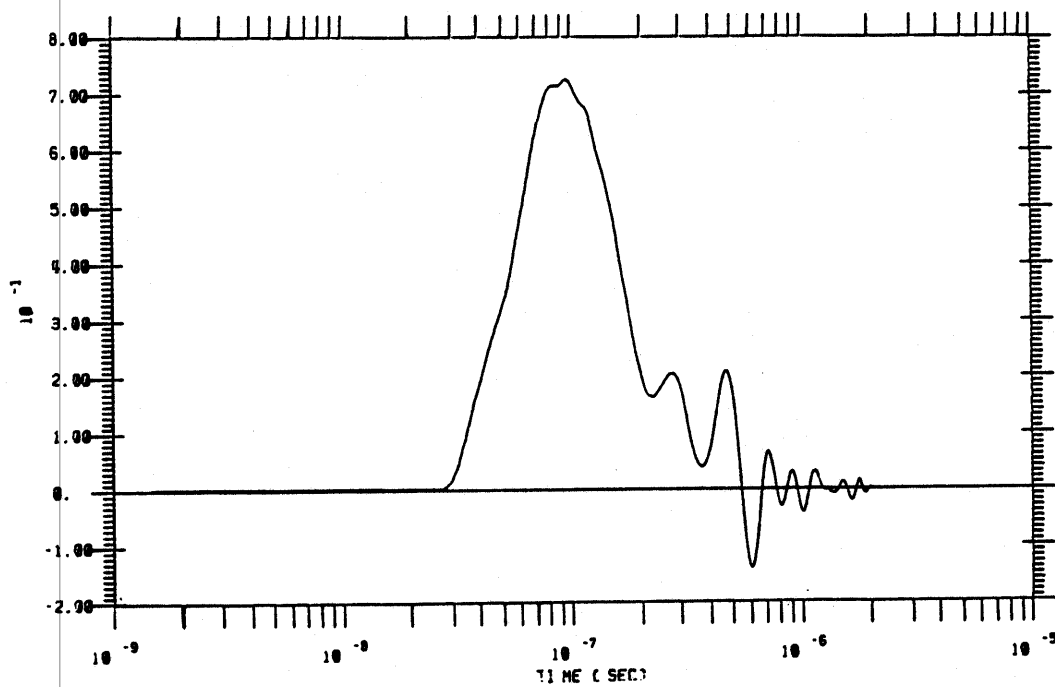Figure 32a. V_{oc} for Measured Effective Height (Horizontal Polarization)

Figure 32b. V_{oc} for Measured Amplitude and Calculated Phase (Horizontal Polarization)
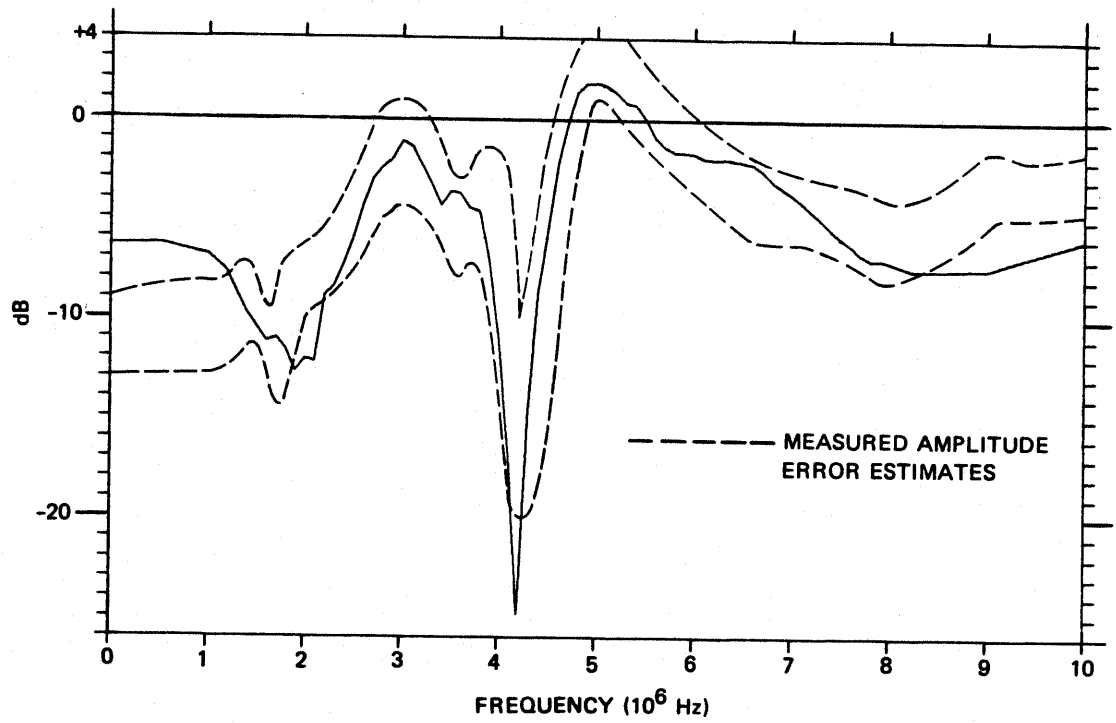
68

Figure 33a. 45° Polarization Calculated Amplitude (10 MHz)
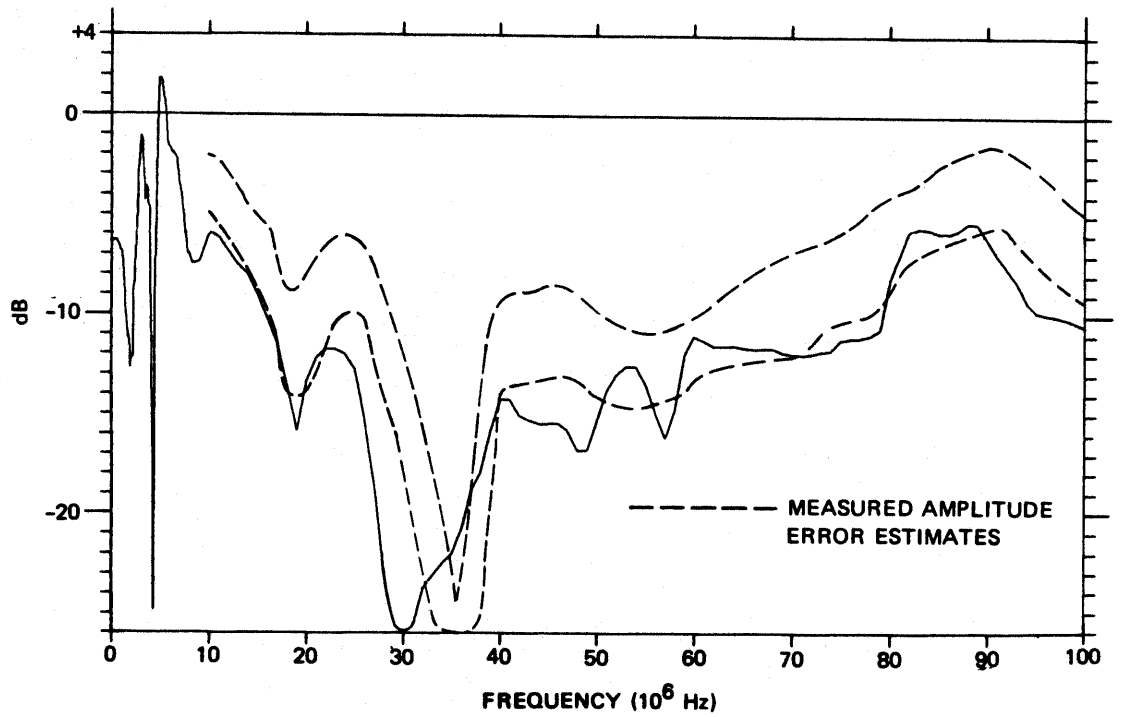

Figure 33b.   45° Polarization Calculated Amplitude (100 MHz)
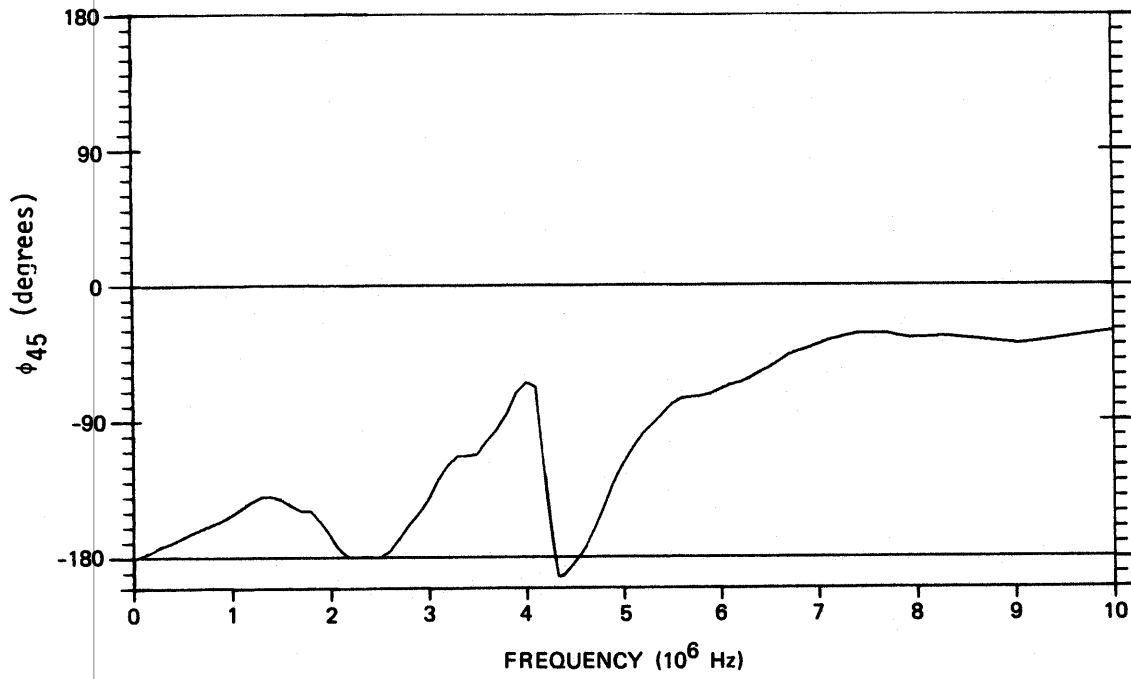
69

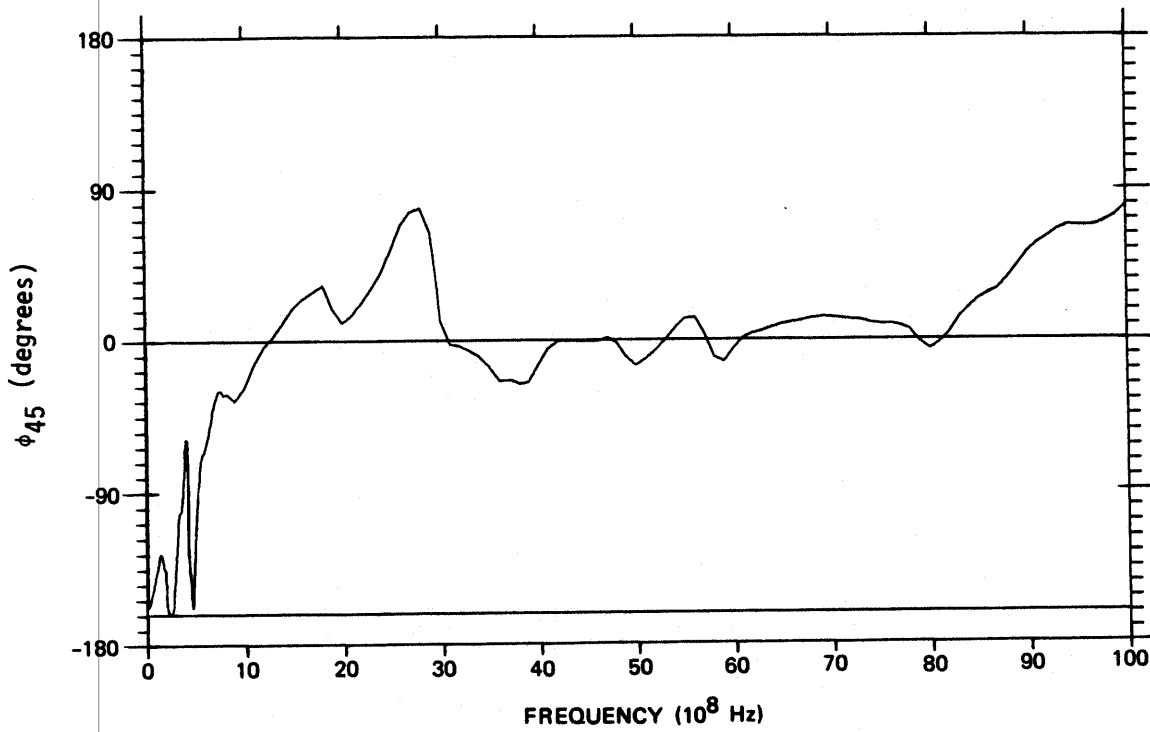Figure 34a.   45° Polarization Calculated Phase

Figure 34b.   45° Polarization Calculated Phase

of the shape of the amplitude curve. However, it can be seen that the curve is outside the measured error bounds particularly from 0-1 MHz where it is higher and above 40 MHz where it is lower. Also, note that there is a calculated null on 30 MHz where the measurement shows a null mean 35 MHz. Before showing any conclusions, a brief discussion of combining errors is in order.

If we combine two quantities which have uncertainties associated with each, then the uncertainty on the combined quantity will be at least as large as the individual uncertainty but can be considerably larger. For the curve at hand, let us consider only the uncertainty associated with the amplitude and let the true value of the vertical and horizontal effect heights be:

$$|h_v|_t = |h_v| \ (1 \pm \varepsilon)$$

and
$$|h_h|_t = |h_h| \ (1 \pm \varepsilon) \ .$$

(62)

Now, if both quantities were in error by a constant bias, i.e., if both had the same sign of an ε, then it can be shown that

$$|h_{45}|_t \simeq |h_{45}| \ (1 \pm \varepsilon)$$

i.e., that the error on the 45° amplitude would be the same as for the horizontal and vertical. However, if the two quantities had different errors, i.e., if the sign of ε for the vertical and horizontal were different, then it can be shown that

$$|h_{45}|_t \simeq |h_{45}| \ \left\{ 1 \pm \cos(45°) \cdot \varepsilon \cdot \frac{\left(|h_v|^2 - |h_H|^2\right)}{|h_{45}|^2} \right\} \ .$$

(63)

71

Thus, the error could be larger for the combined value than on the input values.

For example, consider the quasi-static region (0-1 MHz). In this region

$$|h_v| = 0.45 \text{ or } -7 \text{ dB}$$

$$|h_v| = 1.12 \text{ or } 1 \text{ dB}$$

$$|h_{45}| = 0.47 \text{ or } -6.6 \text{ dB.}$$

Let us now consider the measurement accuracy as ± 2 dB ($\sim 20\%$). If the vertical and horizontal were both in error by ± 2 dB, then from Equation 62 the error in $|h_{45}|_t$ would be

$$|h_{45}|_t = -6.6 \text{ dB} \pm 2 \text{ dB.}$$

However, if the errors on the vertical and horizontal data were not the same but at the extremes of the bands, then

$$|h_{45}|_t = -6.6 \text{ dB} \pm 5.4 \text{ dB.}$$

Note that the increase in the combined error as shown in Equation 63 only occurs when the two quantities being combined are near the same magnitude. When one term dominates, then Equation 63 reduces to Equation 62. Thus for the calculated amplitude of the 45° effective height if one considered the additional errors associated with combining two uncertain quantities, the comparisons would be in reasonable agreement.

The phase data shown in Figure 34 has the properties of changing from -180° to 0° discussed previously.

72

REFERENCES

B-1. Antenna Effective Length Meaurement, The Boeing Company, Seattle, Washington, DNA 3798F-1, 2, July 1975.

B-2. Letter from D. D. Connell (Boeing) to Major W. Adams (DNA) dated 23 September 1975.

B-3. Antenna Effective Length Measurement, The Boeing Company, Seattle, Washington, D180-18878-1, 2, July 1975 (draft).

APPENDIX C.

EFFECTIVE HEIGHTS FOR ANTENNAS ON CONDUCTING SURFACES

The effective height of an antenna is a function which relates the free space electric field with the equivalent open circuit voltage that drives the antenna. In the frequency domain, the effective height can be written as:

$$h_e(\omega) = \frac{V_{oc}(\omega)}{E(\omega)} \, . \tag{64}$$

For a voltage measured across a load, the equivalent circuit would be

$$V_{oc} = h_e \cdot E$$
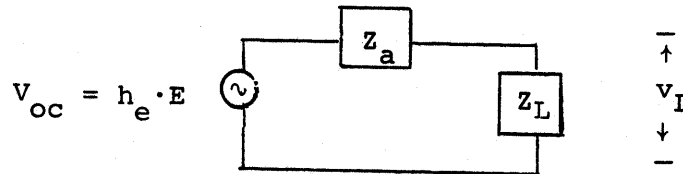
where Z_a is the antenna impedance

Z_L is the load impedance

V_L is the voltage drop across the load.

Thus, if one knows the impedances, the load voltage, and the effective height, then one can determine the external field. However, there is a difficulty which has been evident in a number of experimental measurement programs concerning the estimates of antenna effective heights for a monopole over a conducting ground plane.

Electrically, a monopole antenna over a conducting ground plane is equivalent to a center fed dipole in free space. Figure 35 shows this correspondence. Now, for a dipole it is easy to show that in the low frequency limit, quasi-static, $h_e = L$ where $2L$ is the total length of the dipole. Therefore, an incident field of E_o will produce a voltage drop across the gap of $E_o \cdot L$. To show this, we note that the voltage drop across both the upper and lower halves of the dipole will be $E_o \cdot L$. However, since all points in the upper or lower halves must be at the same potential, in the low frequency limit, the potential for the upper half would be $E_o \cdot L/2$ while for the lower half, it would be $-E_o \cdot L/2$. Their difference, which represents the voltage drop across the gap, is

75

$$V_g = (E_o\ L/2) + (E_o\ L/2)$$

or $\qquad V_g = E_o \cdot L.$ (65)

Now, for a monopole for length L over a conducting plane as shown in Figure 35, the electrical situation is the same as for the dipole except the voltage we want is now the voltage drop across half of the gap. Therefore,

$$V_g = \frac{1}{2}(E_o \cdot L) = E_o \cdot L/2.$$ (66)

It is important to note that in Equation 65, E_o represents the incident free field; however, in Equation 66 E_o represents the total field. The difference is caused by the presence of the conducting ground plane and may be clarified by the following illustration. Consider a plane wave which is incident on an antenna on a ground plane as shown in Figure 36. The normal component of the incident field is $E_n = E_f \cos \alpha$; however, the normal field on the surface of the conducting ground plane is twice the incident field or in our notation

$$E_o = 2 \cdot E_n = 2 \cdot E_f \cos \alpha.$$ (67)

Now, as $\alpha \rightarrow o$, $E_o = 2 \cdot E_f$. Therefore, is we are defining the effective height to be the relationship between the open circuit voltage and the free field, then for a monopole antenna over a ground plane, the effective height (h_e) at low frequencies is not L/2 but L. Thus care must be taken to insure which quantity we are specifying since both of the following equations are true.
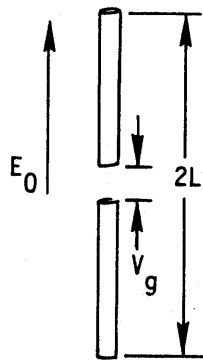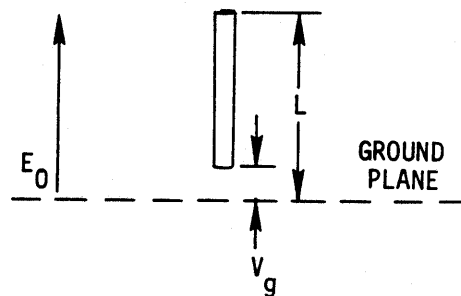
$$V_g = E_o \cdot L/2$$ (68)

and

$$V_g = E_f \cdot L.$$

This same situation of the enhancement of the normal component of the electric field occurs when the antenna is on a conducting cylinder. Consider the geometry shown in Figure 37.

For low frequencies we can approximate the field along the antenna as

DIPOLE   MONOPOLE OVER GROUND PLANE
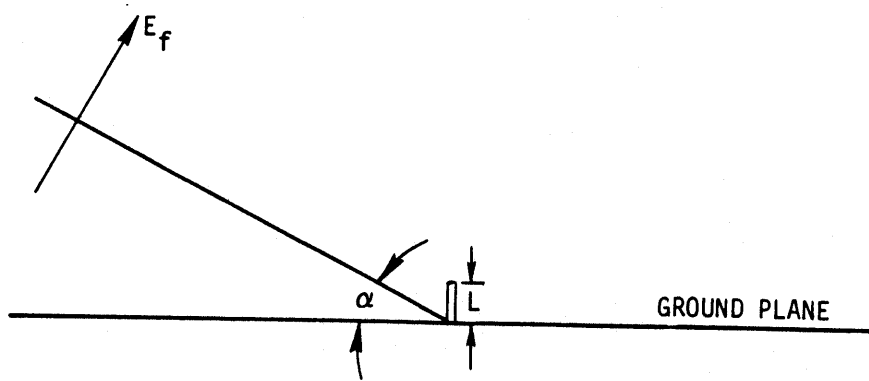
Figure 35. Dipole and Monopole Over Ground Plane
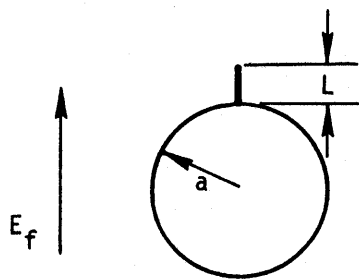
Figure 36.   Incident Field on a Monopole Antenna

Figure 37.   Incident Field on an Antenna Mounted on a Cylinder

$$E_o \simeq E_f \left(1 + \frac{a^2}{r^2}\right) .$$ (69)

Thus, the open circuit voltage for $L/a < 1$ would be approximately

$$V \simeq E_f \cdot L \left(1 - \frac{L}{2a}\right)$$ (70)

and the effective height is

$$h_e \simeq L \left(1 - \frac{L}{2a}\right) .$$ (71)

Again, the effective height is larger than the value of $L/2$ commonly attributed to a monopole over a ground plane with this difference or "enhancement" caused by the difference between a free field and the normal field on a conducting surface.

One final point should be made concerning the effective height for an antenna on a finite length conducting cylinder. Again, we will only consider the low frequencies. As shown in Figure 38, for an incident vertical electric field, the charge distribution on the cylinder caused by the field enhances the local normal field. For an antenna in the center of the cylinder, the net field created by the charges on either side will be aligned along the antenna in the center of the cylinder, the net field created by the charges on either side will be aligned along the antenna and then one would expect an effective height as given by Equation 71. However, as the antenna is moved toward either end, the charge distribution is no longer symmetric; and thus, the net field direction is not aligned with the antenna and the effective height will be less than that given in Equation 71.

If there is a horizontal component of the incident field as shown in Figure 39, then the charge distribution will create electric fields with the polarization shown. For an antenna at the symmetric center of the charge distribution, the election field will be perpendicular to the antenna and there will be no coupling. However, for an antenna located near either end, the electron field will have a component along the antenna but the sign of the induced voltage will change from one end to the other.
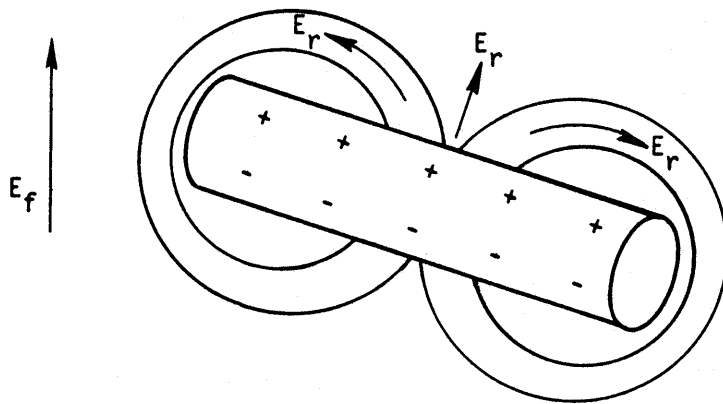
Figure 38. Electrostatic Field from a Finite
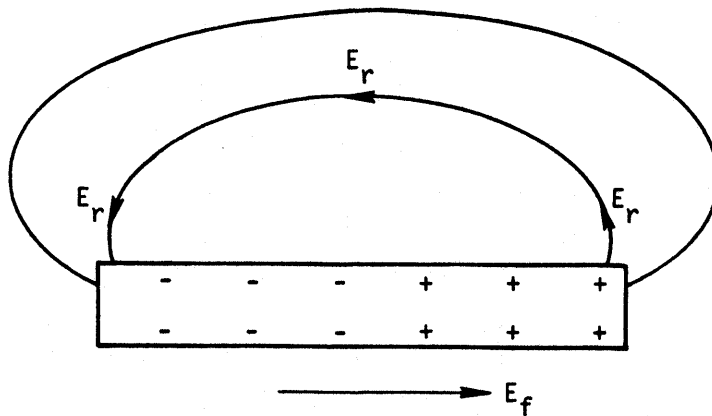Cylinder in a Vertical Field

Figure 39. Electrostatic Field from a Finite
Cylinder in a Horizontal Field

80